Master's thesis

2020

Eirik Haugen

NTNU
Norwegian University of
Science and Technology
Faculty of Information Technology and Electrical
Engineering
Department of Electric Power Engineering

Master's thesis

Eirik Haugen

Optimization of battery energy storage system: A case study for an electric vehicle fast-charging station

June 2020

NTNU
Norwegian University of
Science and Technology

NTNU
Norwegian University of
Science and Technology

NTNU
Norwegian University of
Science and Technology

Optimization of battery energy storage system: A case study for an electric vehicle fast-charging station

Eirik Haugen

Master of Energy and Environmental Engineering
Submission date: June 2020
Supervisor: Magnus Korpås, IEL
Co-supervisor: Kjersti Berg, SINTEF Energy Research

Norwegian University of Science and Technology
Department of Electric Power Engineering

Summary

The increasing fraction of electric vehicles and their charging power, as well as the development of fast-charging stations, creates grid challenges regarding increased peak power and more power fluctuations. The combination of growing charging power, consequently decreasing charging time, gives higher variations. To postpone grid investments by installing stationary battery storage is an alternative to meet increased EV charging demand. The battery storage can peak shave and then fulfill the purpose of avoiding grid reinforcement. This thesis performs a case study of an EV fast-charging station with stationary battery storage to postpone grid investments in case of increased EV charging demand.

The EV charging demand is generated based on stochastic variables and empirical data. Information from a real fast-charging station in Trøndelag, Norway, is used to estimate the EV charging demand at a given fast-charging station. The operation of the fast-charging station is optimized using Julia for a five year period. The operational constraints include the degradation of the battery's capacity, so with time and use, the battery will have a reduced ability to peak shave because of energy storage fade. The optimal battery storage is 225 kWh and 300 kW in the case study.

The results of the case study show no economic arguments to invest in battery storage. The case was not the most suitable for battery storage integration. A situation where potential grid investment costs are higher can give a completely different outcome, for instance, if long power lines need to be upgraded. The investment analysis shows that investing in battery storage to peak shave has 7.5 % higher discounted costs than reinforcing the grid. It also shows that given a higher power tariff, investing in battery storage is not less costly than reinforcing the grid, but the gap between the options contract with 29 %.

More sensitivity analyses are done, including on time step. Through the whole Master's thesis, the time resolution is in minutes for power and degradation. By optimizing the operation of battery storage without degradation, the operational costs are 14.5 % higher if the time resolution is in minutes compared to hours. If cyclic aging, degradation based on the operation of the battery, is included, the cyclic degradation is 45 % higher if the time resolution is in minutes compared to hours.

If projections on future battery investment price for 2025 is correct, the investment cost of the optimal battery is reduced by 31.5 %. Investment reduction gives enormous impacts on the profitability of applying battery storage compared to grid reinforcement.

Sammendrag

Stadig økende andel elbiler og ladeeffekt, samt utbygging av hurtigladestasjoner, skaper nye utfordringer, blant annet økte effekttopper og mer varierende effekt. Med økende ladeeffekt vil ladetiden gå ned, og kombinasjonen av økt effekt og kortere ladetid gir mer fluktuerende laster. For å utsette eller unngå nettinvesteringer kan et stasjonært batterisystem være et alternativ. Batterisystemer brukes til å kutte effekttopper for å holde effekten fra nettet nede på et gitt nivå med formål å unngå oppgradering av eksisterende nett. Denne masteroppgaven ser på en hurtigladestasjon i kombinasjon med et stasjonært batteri for å utsette nettinvesteringer ved økt ladebehov.

Hurtigladestasjonen er stokastisk modellert med forventningsverdier og parametere basert på en reell hurtigladestasjon. Driften av hurtigladestasjonen er optimert i Julia for en fem års periode. I formuleringen av optimeringsproblemet er degradering av batteriets energikapasitet tatt med i de driftsrelaterte variablene. Det vil si at med tid og bruk, vil batteriet ha en redusert tilgjengelig energikapasitet til å kutte effekttopper. Det optimale batterisystemet viser seg å være 225 kWh og 300 kW.

Resultatene viser at det ikke er økonomisk gunstig å investere i et batterisystem i dette tilfellet. Case studiet var ikke det best egnede caset for å se lønnsomhet i en batteriinvestering, men for andre energikonsumenter får man et helt annet resultat - for eksempel dersom lange kraftlinjer måtte oppgraderes. Investeringsanalysen viser at de totale diskonterte kostnadene ved å investere i et batterisystem og drifte det i fem år er 7.5 % dyrere enn å utvide nettkapasiteten. Dersom effekttariffen øker, viser beregningene at det å investere i et batterisystem er fortsatt dyrere sammenlignet med nettutvidelse, men at forskjellen mellom de to alternativene reduseres med 29 %.

Flere sensitivitetsanalyser enn på nettleien er gjort, blant annet på valget av tidssteg i optimeringen. I masteroppgaven er det hele tiden brukt minutt som oppløsning på effekt og degradering. Ved optimering av batteriets drift uten å ha med degradering blir driftskostnadene 14.5 % høyere dersom man bruker tidssteg i minutt i stedet for timer. Dersom man tar med syklisk degradering, altså degradering fra batteriets bruk, går den sykliske degraderingen av batteriet 45 % raskere dersom man har minutt i stedet for timesoppløsning.

Basert på projeksjoner for 2025, går prisen på batterier ned, og nedgangen tilsvarer en reduksjon på 31.5 % i investeringskostnader i dette tilfellet. Dette gir store utslag i lønnsomheten ved å ta i bruk batterier sammenlignet med nettinvesteringer.

Preface

This thesis marks my completion of a Master in Science of Energy and Environmental Engineering at the Departement at Electric Power Engineering at NTNU. I would never have been without the four years in Trondheim and the exchange year in Zürich.

I will give many thanks to my supervisor Magnus Korpås at NTNU for excellent guidance and valuable input. Magnus has a lot of experience in optimization and battery storage, and I am grateful for his answers to my consecutively questions and problems. I would also like to thank my co-supervisor, Kjersti Berg, at SINTEF Energy Research for sound advice and guidance. Kjersti is good at looking at the whole picture, which kept me away from taking side roads. Their guidance and support have been deeply appreciated and have been essential for my motivation and working spirit.

I will thank my family for enormous support, not only the last semester but over all the years of my study. In the end, I also want to thank you, my fellow students, friends, and roommates for an excellent student period with a lot of enjoyable experience.

Trondheim, June 2020

Eirik Haugen

Table of Contents

List of Tables

List of Figures

Abbreviations

EV	–	electric vehicle
PHEV	–	plug-in hybrid vehicle
GHG	–	green house gas
RES	–	renewable energy production
BESS	–	battery energy storage system
PV	–	photovoltaic
FCS	–	fast charging station
DSO	–	distribution system operator
NPV	–	net present value
SEI	–	solid electrolyte interface
SoC	–	state of charge
SoH	–	state of health
DoD	–	depth of discharge
FEC	–	full equivalent cycle

DC	–	direct current
AC	–	alternating current
PLL	–	phase locked loop
PI	–	proportional integral
BMS	–	battery management system
EOL	–	end of life

Chapter 1

Introduction

1.1 Motivation and background

Norway and several other developed countries undergo electrification of many different sectors at a high pace, and new challenges occur from a grid perspective. The Norwegian regulator (NVE) estimates that the yearly energy consumption from electricity will increase from 118 TWh in 2020 to 128 TWh in 2030 [1]. However, the increase in energy is not the problem; the power line capacities and voltage levels in weak grid points are of deeper concerns [2]. Peer to peer, new measuring pieces of equipment, load shifting, and local storage and production are all important elements in the development of meeting these challenges. Grid reinforcements are necessary to meet the new demand. However, new solutions with lower costs and increasing flexibility are also important to consider.

The electrification of the transportation sector is maybe the most relevant example. By an increasing fraction of electric vehicles (EV) and plug-in hybrid electric vehicles (PHEV), the need for electrical power increases in this sector. From a climate perspective, an increasing fraction of EVs is a positive development if the power system is environmentally friendly. An environmentally-friendly system has low greenhouse gas (GHG) emissions from electricity production and EV production [3]. That is why the reinforcement of renewable energy sources (RES) is an important issue as well to make the power system ready for increased energy demand.

A battery energy storage system (BESS) is a potentially important part of the future power system. BESS can serve as a buffer for local production, contribute to frequency control, or as an alternative to grid reinforcement. BESS can do peak shaving, which means that

the BESS provides energy when the demand is high and charge when the load demand is low and most preferably when prices are low. With more local PV production, production uncertainties from increased RES, and higher power at the load side, the relevance of BESS increases [4].

There exist some advantages to using lithium-ion battery cells in a BESS. The self-discharge rates are low, the energy density is high, and the power it can provide is high [5]. A challenge with using this in real life is high prices. For the last years, the prices on lithium-ion batteries have decreased continuously [6], and the research publications connected to lithium-ion batteries are exponentially increasing [7]. Lithium-ion batteries are well suited for large scale grid applications from a technical perspective [8]. For every year that passes, its relevance also increases from an economic perspective, due to decreasing prices.

There have been similar studies having some of the same objectives as this thesis. Fast charging stations with BESS for EVs with a focus on battery degradation and optimal integration into the grid have been an object for earlier research [9, 10]. Article [9] investigates BESS sizes of 250 and 650 kWh with respectively 250 and 650 kW with an assumed battery price of 250 €/kWh and 200 €/kW. FCS is causing negative impacts on the grid in the future with short but high power peaks. If the FCS operator, which installs a BESS, in addition to peak shave, provides ancillary services, the revenues will increase [9]. The installation of BESS has positive effects from a grid perspective. However, the investments needed are still too high, and a battery price reduction of 30 % is required to have a profitable case of a stationary battery [10].

A Master's thesis from 2018 [11] conducts an optimization of installing battery storage of 150 kWh for a medium-scale swimming facility in Norway with an on-site PV production. The optimization included battery degradation as cost element in the objective function and not in the operational constraints, as for instance in article [9] and [10]. By including the degradation as a cost element is a shortcoming in the conclusion of the thesis [11]. The thesis concludes that there is a net saving of 0.64 % of the annual system costs with the BESS installation and a peak power reduction of 13.9 %. Another conclusion is that the system cost is more sensitive to changes in the power tariff than in the battery investment costs [11].

From a system perspective, the degree of flexibility at EV charging infrastructure depends on the management and control of the charging [12]. For instance, energy storage and use of EVs for increasing the flexibility of the power grid requires a smart and well-controlled charging and battery operation. The recommendations of the report [12] are partly that

- competitive markets should provide flexibility services,

- the flexibility services can be opened if there is a high degree of transparency which can lead to more interaction between the DSO and market participants and
- the DSO should give incentives for conventional grid reinforcements when unconventional solutions are not feasible.

Another recommendation from the report [12] is that the involvement of the DSO in planning the EV charging infrastructure should be only in a stage where the market is immature. In advance of the time when the market is mature, the report highly recommends the DSO to have a clear exit strategy for the involvement in EV charging infrastructure [12].

1.2 Problem description

Electrification leads to increased demand for electricity in several sectors, including the transportation sector. The traditional approach of reinforcing the existing grid is an alternative to install a stationary BESS to shave power peaks. Commercial customers of the grid must pay a fee for the monthly power peak to the distribution system operator. If the peak power is high, the customer has incentives to reduce it to save costs.

Fast charging stations for electric vehicles are in such a situation when the amount of fast chargers increases. Load shifting is not a possibility because the operator of the fast-charging station cannot control when cars are coming in. With a battery storage system, the operator can store energy for the busiest time periods and thus keep the grid power below a desired limit. This peak shaving technique can generate cost savings, which in turn pays down the investment of the BESS.

By conducting a case study of a fast-charging station, the goal is to compare a battery installation to reinforce the grid and determine which investment alternative makes the most economic sense. The method is to create an optimization model, which minimizes the overall costs for the fast charging station operator. The optimization model will include battery capacity degradation. Sensitivity analysis shows how the impact of different parameters, such as degradation, spot price, grid tariff, and the time step, have on the system.

There are several important notes to make, which regards the details of the total description. First, the battery degradation should be well-considered and incorporated into the optimization. The reason for this is to have a real-life analysis that takes as many influencing factors as possible into account. Instead of estimating degradation as a pre-calculated equivalent cost based on previous simulations, it is in the operational constraints. The battery capacity will become lower by time and use, and the grid must provide a continuously increasing amount of energy.

Second, the load increase is an EV charging demand at a fast-charging station (FCS) based on stochastical distributions and empirical data. The modelled EV charging demand, which is the case study, is based on detailed information handed in from Tensio for a specific and anonymous FCS in Trøndelag. Tensio is the DSO in the Trondheim area. To sum up, the candidate shall

1. optimize battery size and costs of applying BESS at an EV FCS if the number of charging points increases with 50 %
2. compare installation of BESS to grid reinforcement in the case study
3. look into advantages and disadvantages for the DSO when a consumer applies BESS to peak shave, based on the case study and sensitivity analysis
4. include battery degradation in the optimization model
5. explain fundamental effects and mechanisms of battery degradation
6. analyze the impacts of including battery degradation in the analysis
7. perform sensitivity analysis on the spot price, power tariff, and time step.

1.3 Approach

The optimization model is build up by a mathematical formulation of equations and constraints based on operational and system properties and characteristics. The optimization problem is written in Julia using the JuMP package and solved by the optimization tool solver Ipopt. The load demand, which is input, is generated by a method developed by the author in the specialization project during fall 2019. In general, the method used to find the best solution is as follows

1. Determine the EV charging demand at the FCS. The basis for modeling an EV charging demand is from the specialization project during the fall [13], and further changes are presented in section 3.3. The input is information about a particular EV FCS, given from Tensio, such as the number of chargers and maximum power.
2. Establish case. Section 4.1 establishes a case where a comparison of grid reinforcement and BESS installation.
3. Decide on which cost elements which should be in the objective function. Based on that, formulate a cost function that will be the objective function, and minimized in the optimization. The objective function is deducted and presented in subsection 3.2.1.

4. Set up the constraints for the case and then the overall mathematical formulation. The constraints are set up in subsection 3.2.2 and the mathematical formulation for the optimization problem is shown in subsection 3.2.3.

5. Decide the value of the economic parameters, such as grid tariffs, electricity price, investment costs, discount rates, and degradation costs. The values for the case study is summarized in section 4.3.

6. Choose a proper solver to solve the formulated optimization problem. Important issues are complexity, i.e., non-linearities, and size. Section 3.4 discuss and explain the choice of solver, as well as describing the implementation.

7. Compare the financial results between BESS installation and grid reinforcement and realize the most economically reasonable option. The results are presented in section 5.1, discussed in section 6.1 and concluded in section 7.1.

1.4 Structure

First, this introduction is presenting the motivation and literature background, problem description, approach, and structure of the report. The content of the remaining chapters is summarized below.

Chapter 2, *Literature and theory*, introduces the theory of fundamental lithium-ion battery storage technology and degradation, optimization, economic analysis, and error estimation.

Chapter 3, *Method*, presents the methodology for BESS optimization and EV charging demand estimation.

Chapter 4, *Case study*, contains the results from modeling EV charging demand at the FCS. The case study is formulated with the modeled EV charging demand. The estimated charging demand is input to the optimization model.

Chapter 5, *Results from case study*, presents the result of the case study, which is a comparison between the optimized BESS and grid reinforcement. The chapter contains results from degradation analysis and sensitivity analysis on spot price selection, grid tariffs, and time steps.

Chapter 6, *Discussion*, discuss the findings and results presented in the chapter 5.

Chapter 7, *Conclusion and further work*, concludes on the working points described in the problem description based on the results and discussion. Suggestions for further work are presented.

.

Chapter 2

Literature and theory

This chapter starts with laying a theoretical background for lithium-ion battery technology and degradation. Then the chapter introduces net present value, investment analysis, general optimization setups, and error estimation.

2.1 Battery energy storage system

Lithium-ion batteries are globally increasing both in installed capacity and market shares. In 2011, the total capacity addition of lithium-ion batteries was 25 MW globally and 40 % of the total capacity addition market [14]. Five years later, in 2016, the global capacity addition of lithium-ion batteries had increased to 162 MW and a market share of almost 90 % [14]. The last 10 % contains lead-acid batteries, sodium-sulfur batteries, and others.

2.1.1 Battery fundamentals

A BESS consists of many modules, which in turn include battery cells. The battery cells, which in this case are lithium-ion based electrodes, consists of a cathode (positive electrode), an anode (negative electrode), an electrolyte, and a separator. The electrodes and the separator is in the electrolyte, and the separator is there to insulate the electrodes and only allow ionic transport of lithium ions.

Table 2.1 shows the most typical lithium-ion batteries, and their cathodes and anodes, as well as the standard, used abbreviations for each type. Usually, for lithium-ion batteries, the cathode is lithium oxide, and the anode is graphite. For LTO, this is not the case, be

aware that the lithium titanate oxide is the anode of the battery.

Table 2.1: Abbreviations for different lithium ion battery technologies.

Battery cathode	Battery anode	Abbrev.
lithium cobolt oxide	graphite	LCO
lithium manganese oxide	graphite	LMO
lithium nickel manganese cobolt oxide	graphite	NMC
lithium iron phosphate	graphite	LFP
lithium nickel cobolt aluminum oxide	graphite	NCA
lithium manganese oxide	lithium titanate oxide	LTO

Further, the different batteries with different cathodes perform differently and have different strengths and weaknesses. For selecting the best battery configuration and also the rates of degradation, it highly depends on the chemistry of the battery [3]. NCA is the best performing cathode on lifetime, while LFP, NMC, and LMO-NMC show high sensitivity on temperature [3].

Table 2.2: Characteristics for different cathodes in lithium ion battery cells.

Abbrev.	Charge [C]	Discharge [C]	Lifetime (FEC)	Specific energy [Wh/kg]	Thermal runaway[°C]
LCO	0.7-1.0	1.0	500 - 1000	150 - 200	150
LMO	0.7-1.0	1.0	500 - 5000	100 - 150	250
NMC	0.7-1.0	1.0	500 - 5000	150 - 220	210
LFP	1.0	1.0	1000 - 10000	90 - 130	270
NCA	0.7	1.0	500 - 2000	200 - 260	150
LTO	1.0	10.0	5000 - 10000	70 - 85	-

According to [15], LTO and LFP are the lithium-ion cathodes that have the highest performance for BESS operation. Because of the high titanium costs, selecting LFP will give lower investment costs than LTO. Regarding other characteristics for LTO and LFP, they are quite similar, which includes energy density, power density, safety, and lifetime.

Different degrees of the described degradation mechanisms depend on what cathode it is. The constants during the process of making the constraints reflect the differences.

It is necessary to connect a AC/DC converter (rectifier) between the BESS and the load bus when connecting BESS at a AC load bus. If the load bus is a DC bus, a DC/DC converter is necessary. Fast chargers for EV applications are in almost every case DC chargers. Each charger is connected to the DC bus with a DC/DC converter, as well as the BESS. A conventional, uncontrolled rectifier may give power quality problems on the grid side due to the presence of current harmonics and voltage distortion [16]. There exist limits on minimum allowed power factor, and converter control of the rectifier with PLL and PI control of the DC voltage is necessary [16]. The current and voltage are properly controlled with PLL and PI control [17].

2.1.2 Degradation mechanisms for lithium-ion batteries

Battery degradation has an impact on the economic outcome that looks at BESS operations. A techno-economic analysis, as in Naumann's Ph.D. thesis from 2018 [18], consider an analysis where technical and economic aspects are combined.

Degradation mechanisms in lithium-ion batteries depend on operation and storage conditions. The effects of degradation consist of two separate effects. The first is energy storage capacity loss, referred to as capacity loss. The second one is reduced power the BESS can supply, referred to as power fade. State of health (SoH) and internal resistance R_{int} represent the two degradation effects. The instantaneous battery energy capacity, $E_{B,cap}$, which is the maximum energy the battery can store compared to the initial storage capacity, E_{B0}, is represented by the SoH. SoH is a percentage that is continuously decreasing as a consequence of degradation mechanisms caused by time and use of the battery. Mathematically it is formulated as [18]:

$$E_{B,cap}(t) = SoH(t) \cdot E_{B0} \tag{2.1}$$

Typically, when the SoH is 80 %, it is considered as the EoL criterion and initiates a reinvest because then the BESS is considered to be unusable [19]. By the car industry, the EoL is set to between 70 and 80 % [9]. The origin of this limit is from lead-acid batteries, which experienced a rapid decrease in capacity after the SoH decreased to 80 % [20]. For lithium-ion batteries, the EoL criterion can be lower. Typically, stationary applications such as BESS exploits previously used batteries. There is no adequate method or understanding of how batteries below 80 % should operate, and the degradation is perhaps following different patterns [21]. However, a residual value can be assumed by stating that batteries with SoH below 60 % can not operate.

SoC is the instantaneous percentage of energy level of the BESS, mathematically formulated as [18]:

$$SoC(t) = \frac{E_B(t)}{E_{B,cap}(t)} \tag{2.2}$$

SoC increases when the BESS charges and decreases when the BESS discharges. For various reasons, for instance degradation, the SoC is limited by a lower and upper boundry, formulated as:

$$SoC \geq SoC_{min} \tag{2.3}$$

$$SoC \leq SoC_{max} \tag{2.4}$$

Calender aging mechanisms

Calender aging is an unavoidable battery capacity reduction as a function of time. There have been several experimental studies that looked into the impact on degradation from the battery storing conditions. It shows that the temperature is the primary factor for accelerating calender aging, but also the state of charge (SoC) has a massive impact. These variables also influence the self-discharge rate [4].

The primary mechanism which causes degradation is the growth of a solid electrolyte interface (SEI). A high SoC, which is equivalent to a high voltage difference between electrodes, accelerates the degradation since the difference in electrode potentials is important [4]. There is a clear consensus that SEI growth dominates calender aging. By Arrhenius relation, the capacity decrease due to calender aging has an underlying time dependence as $\sqrt{t}$. The BESS capacity E_B reduces over time corresponding to SoH, which represents the capacity fade. Besides, several minor degradation mechanisms are working on various battery components and result in capacity and power fade.

Cyclic aging mechanisms

Cyclic aging is degradation caused by the operation of the battery. Here, two significant effects are highlighted because they are particularly impacting the rate of power fade and capacity fade [3]. The first is lithium plating which leads to both capacity fade and power fade. Temperature and C-rate are the main drivers for this effect. The second is a mechanical failure, which causes both capacity and power fade. A mechanical failure at the

cathode is just driven by DoD. At the anode, C-rate, SoC, and DoD impact the mechanisms. A full eqvivalent cycle (FEC) is when the change in SoC correspond to one cycle between the minimum SoC and the maximum [18]:

$$FEC(t) = \frac{1}{2}\int_T \left|\frac{\partial SoC(t)}{\partial t}\right| SoH(t)dt \tag{2.5}$$

$$= FEC(t-1) + \frac{1}{2}\cdot\frac{|SoC(t) - SoC(t-1)|}{SoC_{max} - SoC_{min}} \tag{2.6}$$

$$= FEC(t-1) + \frac{1}{2}\cdot\frac{P_{char}(t) + P_{dchar}(t)}{E_{B0}\cdot(SoC_{max} - SoC_{min})}\cdot\Delta t \tag{2.7}$$

The C-rate with unit $\frac{1}{\mathrm{h}}$ is the rate of which the BESS is charging or discharging. The definition is that 1 C is the rate when the BESS delivers its nominal capacity during one hour. The C-rate is [18]:

$$C_{char}(t) = \frac{P_B(t)}{E_{B0}} \tag{2.8}$$

If the BESS is represented as an equivalent circuit, the internal resistance represents the power fade in the BESS [22]. Over time and by use, the internal resistance will increase due to degradation mechanisms. The currents can be calculated from the charging and discharging power, P_{char} and P_{dchar}. By having R_{int} as a variable representing the power fade, then these equations would be non-linear. The same will be the case for SoH, which gives the currently available energy storage capacity by multiplying SoH with the initial storage capacity. It is not a linear equation nor constraint - two non-linear constraints for each time step origins from these two operating measures for battery degradation.

Figure 2.1 shows the lifetime as a function of temperature. The degradation is, as mentioned, highly dependent on temperature. However, these equations are not linear. The graph in figure 2.1 is the same shape as experiments conducted by several institutions shown in subsection 2.1.2. The right part of figure 2.1, which is increasing due to Arrhenius law, is related to calender aging as the dominant effect. Lithium plating dominates the left and corresponds to accelerated cyclic aging. When the battery has a high C-rate and the cycle degradation is high, the increasing temperature due to high currents and thermal losses decelerating the degradation.

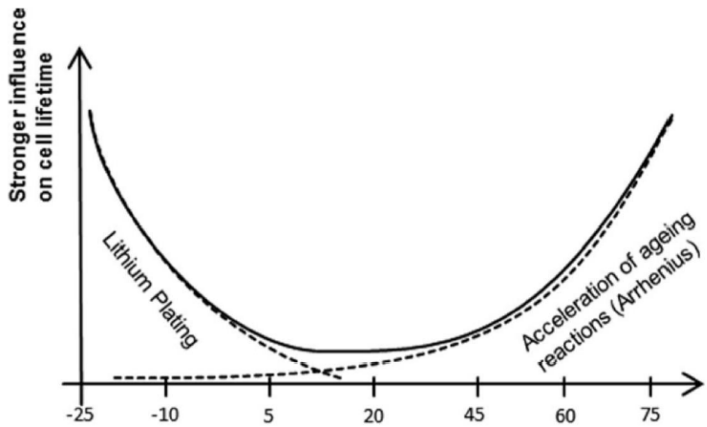

Figure 2.1: Battery life time as function of temperature [21].

Existing models to estimate battery degradation

To model degradation mechanisms, several models are suggested and applied in the later years. This subsection presents four models, where some elements from them are involved in modeling the degradation for the case study. Three of the models have specific names (named as in [3]), NREL, Wang, and MOBICUS, which are semi-empirical and were introduced 6 to 8 years back in time. A more recent and much more detailed model with an experimental basis is from the already mentioned Naumann Ph.D. [18]. The author of the Ph.D. thesis created an objective oriented program in Matlab for his model, called SimSES [23]. The SimSES model is a deterministic operation model with build-in accurate battery degradation which can be run with different applications.

The three first models are very alike and build on each other [3]. The first publication of the NREL model was in [24] and later used to model degradation mechanisms in batteries [3]. The equations for internal resistance increase (power fade) and loss of energy capacity incorporates calender and cyclic aging. The internal resistance in the BESS R_{int} is growing with a rate that consists of two additive terms, one caused by calender aging and one by cyclic aging. The increase in R_{int} is linearly proportional to the number of cycles, FEC, and to the square root of time, $\sqrt{t}$.

$$R_{int} = R_{int}^{init} + a_1\sqrt{t} + a_2 FEC \tag{2.9}$$

According to the same model, the loss of energy capacity depends on the loss of active

lithium or lithium inventory. The minimum of these two is the capacity loss, ΔQ.

$$\Delta Q = min(b_0 + b_1\sqrt{t}, c_0 + c_1 FEC) \tag{2.10}$$

There are one storage and operational condition set for the model. If there are several conditions, predefined factors should be defined as a function of $T, V_{oc}, \Delta DOD$, and more, if possible, to correct the expressions. These equations are not shown here; they are not used in the case study and is highly non-linear. The NREL model includes temperature, SoC, and time in the calender aging equations and temperature, SoC, C-rate, and DoD in the cyclic aging equations. The NREL model is based on lithium-ion batteries with NCA and LFP as cathode [3].

MOBICUS is an abbreviation for modeling of batteries, including the coupling between calender and cyclic aging. The first demonstration of the model equations was in [25] and later used in several papers and projects. MOBICUS can is as an extension of NREL according to [3]. The formula for an increase in internal resistance is the same as in the NREL model given in equation 2.9. MOBICUS assumes that the calender aging dominates the total degradation. The battery capacity decrease in equation 2.10 is

$$\Delta Q = min(b_0 + b_1\sqrt{t}, c_0 + c_1 t) \tag{2.11}$$

The vital change from the NREL model is the change in the cyclic influence represented by FEC to a linear time element t. The MOBICUS model includes temperature, SoC, and time in the calender aging equations and temperature, C-rate, and DoD in the cyclic aging equations. The MOBICUS model is based on lithium-ion batteries with NCA, LFP, NMC-LMO, and NMC as cathode [3].

The model equations for battery degradation given in [26] make the origin of the Wang model. The model describes cyclic aging and capacity fade in NMC and LMO cells, as well as calender aging, which linearly follows the square root of time. The experiments reported in the Wang article show that the predicted degradation estimated by the model corresponds with measured values for 10, 20, 34, and 46 °C [26]. The work done in the original Wang article ([26]), is based on previous work estimating LFP cell's lifetime [3]. The general Wang equations for capacity loss is a sum where the first term is the cyclic degradation and the second term is the calender degradation.

$$Q_{loss,\%} = (a \cdot T_K^2 + b \cdot T_K + c)e^{(d \cdot T_K + e) \cdot C_r} Ah_{throughput} + f \cdot \sqrt{t} \cdot e^{\frac{-E_a}{RT_K}} \tag{2.12}$$

For experimentally purposes, commercially available NMC-LMO battery was used, more specifically a 1.5 Ah, 18650 cylindrical cells (UR18650W) from Sanyo [26]. The results are origin to the Wang model and its constants given in table 2.3.

Table 2.3: Constants in the Wang model.

Name	Value	Unit
a	$8.61 \cdot 10^{-6}$	$1/AhK^2$
b	$-5.13 \cdot 10^{-3}$	$1/AhK$
c	$7.63 \cdot 10^{-1}$	$1/Ah$
d	$-6.7 \cdot 10^{-3}$	h/K
e	2.35	h
f	14.876	$1/\sqrt{day}$
E_a	24.5	kJ/mol
R	8.314	$J/Kmol$

i. C_r is C-rate [1/h]

ii. t is time [days]

iii. T_K is temperature [K]

The power loss is quite low compared to the capacity loss even after several thousands of FEC when the C-rate is under 5C, and the temperature is above and around 20 °C [26]. The Wang model includes temperature and time in the calender aging equations and temperature, C-rate, and, to some extent, DoD in the cyclic aging equations. The Wang model is based on lithium-ion batteries with NMC-LMO as cathode [3]. Cordoba-Arenas et al. [27] propose a similar model for NMC-LMO batteries to Wang's. The cyclic aging is not linear to FEC but linear to FEC to the power of z, where z in the case of NMC-LMO is 0.48, i.e., the square root. A case study that applies the Wang model to EV batteries studies the degradation for various driving distances [28]. There are two notable aspects of the results of the case study in [28]. The first is that NMC-LMO has the best life span of the tested lithium-ion batteries. NCM + Spinel Mn and $LiFePO_4$ where other cathodes, with no predicted end of life (EoL) below six years for NMC-LMO. The second aspect is that compared to experimental test data from EVs, the Wang model overestimates the degradation.

The models have many of the same characteristics and interactions between different states and variables. The Nauman Ph.D. thesis from 2018 is quite more sophisticated and shows

some of the same fundamental relations and even more depending and non-linear relations [18]. Reference [18] reports experiments with 1850 LiFePO4-graphite cells, and it proposes equations for both calender and cyclic degradation. There is energy capacity degradation as a function of three multiplied functions. One is the square root of time, one is a function of temperature (exponential), and one is a function of SoC (SoC to the third). For the cyclic aging, which also is three functions multiplied and one them is the square root of FEC [18]. Not a linear FEC function, as the Wang model suggests. Another of these three functions describing cyclic degradation is including the C-rate, and the relationship is linear, not exponential, as indicated in the Wang model. The last is expressing a relation with DoD, which is to the third and, in other words, highly non-linear.

By combining some of the equations in [18], makes a fundament of establishing a good model. The Nauman Ph.D. proposes a sophisticated model that justifies a linear relation between degradation of energy capacity and C-rate. In section 3.2.2, the exponential function in the Wang model, which includes C-rate in the exponent, is linearized.

The referred studies in the introduction ([9, 10]) have models based on the Wang model. In the optimization for the case study in this thesis, the Wang model will model the battery degradation of the BESS.

Several more simple approaches have been taken and can be sufficient in some cases. A possible way to estimate battery degradation is as the own cost element dependent on various factors. For instance, Kempton and Tomic suggest the equation:

$$c_d = \frac{c_{bat}}{L_{ET}} \tag{2.13}$$

where L_{ET} is the total energy throughput during the battery's lifetime, and c_{bat} is the capital cost of the battery [29]. The factor L_{ET} is equal to $L_c \cdot E_S \cdot DOD$, where L_c is the lifetime of the battery given in cycles, E_S the total battery energy and DOD depth of discharge, at which L_c is determined. Making a reasonable estimate requires that the lifetime is given and independent of use and operation, which is not the case in real life. This way to describe battery degradation provides several advantages, such as smaller optimization problem which requires less computational power. The optimization will be completely linear.

2.1.3 Battery investment costs

In previous work, the battery installation costs have been assumed to be 16 000 NOK/kWh and the annual maintenance costs to be 1 % of the initial investment costs [30]. However,

these cost estimates are conservative and need to be updated. The battery price, which is used in [10], presented in the introduction, is 250 €/kWh plus 200 €/kW.

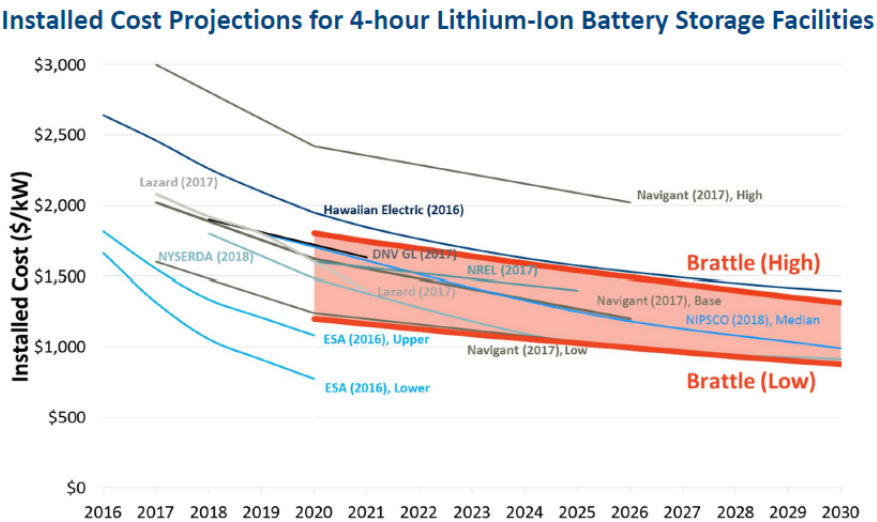

Figure 2.2: Estimates on battery investment cost [31].

To find precise estimates for battery prices are complicated. Because of the rapid decrease in investment costs, figures from just four and five years back can already be outdated. Table 2.4 shows the highest and lowest estimates found for lithium-ion batteries for the years 2018 and 2019. There will be differences in prices because of the different material costs for different battery electrode chemistries.

Table 2.4: Price estimates for lithium ion batteries with exchange rate of 9.5 NOK/USD.

Company	Year	Lowest price [NOK/kWh]	Highest price [NOK/kWh]	Average price [NOK/kWh]
Wood Mackenzie	2018	3990	6175	5083
NIPSCO	2018	3135	7410	5273
EPRI	2018	3040	4940	3990
Brattle	2018	3040	4560	3800
Lazard	2018	2755	3325	3040

There are several cost projections from different sources, and figure 2.2 shows the development and forecast for the cost of lithium-ion batteries in USD/kW [31]. The cost in

USD/kW is meant for a battery operating 4 hours a day, and the price in USD/kW must be divided by 4 hours to get the price in USD/kWh.

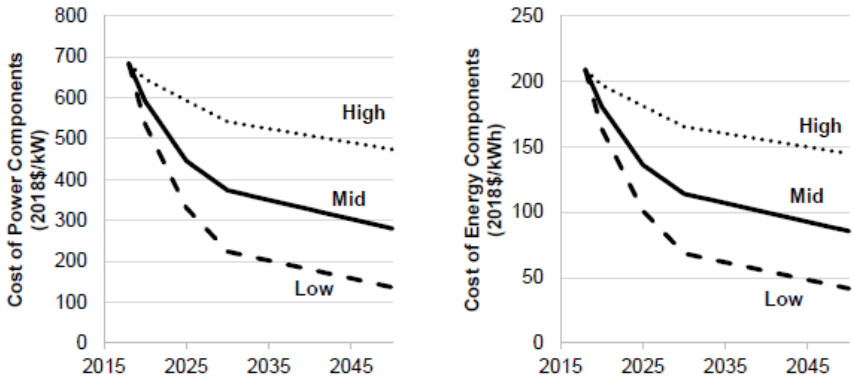

Figure 2.3: Investment cost projections for lithium ion batteries [32].

The investment cost in a battery should be divided into cost per energy unit kWh and cost per power unit kW. The cost element of energy is associated with the cells and battery technology. In contrast, the cost of power is related to the power electronic devices. These two elements are already a part of the objective function defined in subsection 3.2.1. Figure 2.3 shows the estimated projection of these two cost elements regarding the investment of BESS.

Figure 2.3 shows the cost for both the energy and power term based on a major literature review finished in June 2019 by the U.S. national renewable energy laboratory [32]. The estimated costs are then the sum of the BESS power multiplied with the specific price in NOK per kW, and the BESS energy storage capacity multiplied with the specific price in NOK per kWh. The specific cost in USD is for energy storage capacity c_E = 200 USD/kWh and for power c_P = 650 USD/kW. By applying an exchange rate of 8.5 NOK/USD, which was the average rate for the period 2018 to 2019 [33], the specific investment costs for the battery is c_E = 1700 NOK/kWh and c_P = 5525 NOK/kW.

To compare this price with Brettles's literature review for instance, the specific investment cost for the power term, must be divided with 4 hours. Then the specific investment cost in total then becomes $c_{BESS,kWh} = c_E + \frac{c_P}{4h} = 200 + 650/4$ USD/kWh $= 362.5$ USD/kWh = 3081.25 NOK/kWh or per kW with 4 hours operation $c_{BESS,kW} = 200 \cdot 4 + 650$ USD/kW $= 1450$ USD/kW = 12 325 NOK/kW. The cost of 1 450 USD/kW is fitting in the middle of the estimated cost for 2020 shown in figure 2.2 from a literature review by Brettle [31]. The specific cost elements will be multiplied with the resulting maximum BESS power and storage capacity given in the solution of the optimization. The specific

costs are

1. $I_B^{E,cap}$ = 1700 NOK/kWh for energy storage capacity
2. $I_B^{P,cap}$ = 5525 NOK/kW for power capability

This cost element is the most uncertain in this thesis. It is important to specify that, in reality, correct investment costs should be available when a company or DSO does this kind of analysis.

2.2 Optimization

Optimization refers to the situation where an objective function is minimized within a limited space determined by the constraints. In general, an optimization problem is on the form

$$\begin{aligned} \underset{x}{\text{minimize}} \quad & f(x) \\ \text{subject to} \quad & h(x) = 0 \\ & g(x) \leq 0 \\ & x \geq 0 \end{aligned}$$

where $f(x)$ is the objective function and the vector of decision variables is $x = [x_1, x_2, \ldots, x_n]$ [34]. The equality constraints $h(x)$ and inequality constraints $g(x)$ set boundaries of where the feasible region is, a region where the solution must be within. The objective function f is minimized with respect to x inside the feasible region determined by the constraints.

Dual variables

For an optimization problem, dual variables can be calculated by the Lagrange function [35]. The dual variables provides information on how much a change in the corresponding constraints impacts the objective function. The Lagrange function is defined as:

$$L(x) = f(x) + \sum_x \lambda(x) \cdot h(x) + \sum_x \mu(x) \cdot g(x)$$

where λ and μ are the dual variables for, respectively, the equality and inequality constraints. When the Lagrangian function is derivated with respect to all the variables and

set to zero are called Karush Kuhn Tucker conditions. By assuming the problem is linear, linear algebra will give a solution with the value of the dual variables. The derivated expression equal to zero is satisfied for the optimal solution.

$$\frac{\partial L}{\partial x_i} = 0 \qquad \forall x_i \in x \tag{2.15}$$

The dual variables provide numeric information about how a change in the corresponding constraint changes the objective function. For the case of a non-zero dual variable, the corresponding constraint is at its boundary in the optimal solution. When the objective function represents costs and the relevant constraint has a particular unit, the value of the dual variable in the optimal solution is the marginal cost.

2.3 Economic analysis

This section provides background material to understand the economic calculations and various cost elements, such as spot price, grid tariffs, and transformer loss costs.

Net present value

Over time, money loses value. The interpretation of why can be many; however, to discount cash flows, the discounting rate expresses the time value. With a discount rate r, a future value, FV, in year N can be calculated to a present value, PV, by multiplying FV with $\alpha(N)$. Equation 2.16 describes this mathematically [36].

$$\alpha(N) = (1 + r)^{-N} \tag{2.16}$$

The method to calculate the long term economic cost is done by net present value (NPV) in equation 2.17 by applying the discounting term shown in equation 2.16 [36].

$$NPV = I_0 + \sum_{n=1}^{N} \alpha(N) \cdot C_n - R_N \tag{2.17}$$

I_0 - investment cost [NOK]

n - year

N - years of analysis

α - discount factor (defined in equation 2.16)

C_n - cash flow in year n [NOK]

R_N - residual value ind the end of the last year N or beginning of year $N+1$ [NOK]

Equation 2.17 shows the net present value by discounting a cash flow and sum up the initial investment cost and the residual value. The residual value is the remaining value of the investment after the end of the economic period of N years. Further, in this section, a description of some cost elements follows.

Spot price

The spot price is the current price for electricity determined on the market to ensure the balance between supply and demand [37]. The spot price is fluctuating along with the supply and demand changes. Electricity can be bought on the intra-day market and day-ahead market. Other derivates, such as forwards and futures, where the price is locked for future delivery, can be purchased to reduce risk [38].

Grid tariffs

The grid tariffs are the fees a consumer has to pay to the DSO. The grid tariff consists of three parts, the fixed term, the power tariff, and the energy tariff and is known parameters [39]. Some cost parameters are difficult to predict, such as the spot price in the coming ten years and the investment costs. The financial parameters will vary and be estimated differently for different cases.

Tariffs are what companies and households pay to the DSO to use the grid. The grid tariff price levels are based on several factors [40]

- energy consumption, if the DSO does not correctly estimate the consumption, the tariff is adjusted to cover the income difference.
- electricity price, DSO must cover the physical losses in the grid.
- investment and maintenance, the grid is constantly under expansion and maintenance.
- fees, the DSO is obligated to pay some fees to certain public institutions.
- blackouts, DSO is responsible for covering the costs in case of a blackout.
- interest rate, the level of state obligations and dividend depend on this.

Transformer loss costs

The DSO can not own batteries according to Norwegian law [41], which means that the owner of the FCS must operate their own BESS. To secure reliability and power quality, the DSO can make an agreement with a customer with flexible resources. The DSO can, in the agreement, offer reduced grid tariffs in exchange for getting a guarantee that the customer uses the BESS in specified situations. In [42], such a contract is investigated and presents a model that compares customer's cost savings with different pricing schemes. The result leads to postponing of grid reinforcements and improved voltage control [42].

Subsection 4.1 presents the case study, the alternative to not invest in a BESS is that the customer pays for a new, higher rated transformer [39]. In the case study, the cost of strengthening the grid is a cost paid by the customer, because the customer provokes the need for it. The total cost will be the investment itself and the cost of power losses. Power loss costs are the additional loss of the generated electricity, which has a cost equivalent to the electricity production costs for the society [43].

A planning guide published and created by SINTEF Energy Research is useful to make estimates for transformer and substation costs [43]. The planning guide contains equivalent specific costs for investment and power losses, which is found in a table based on the voltage level and rated power capacity. The capitalized costs have a discounting rate of 4,5 % for 30 years and 2014 price level [43]. The calculation of the total losses is with the capitalized factors for losses. The discounted cost elements are, therefore, investments and costs of losses. To discount future values to present values, equation 2.16 is used.

An important variable is the so-called "utilization time for losses" κ_t [hours]. κ_t is the number of hours during a year when the transformer must operate at the power loss at the transformers rated power to cover the annual losses. Mathematically κ_t is [43]

$$\kappa_t = \frac{\Delta W}{\Delta P_{max}} \tag{2.18}$$

where ΔW is the annual energy losses [kWh] and ΔP_{max} is the losses when the transformer is operating at maximum level [kW]. The annual transformer cost of losses, C_{loss}^{tot} is [43]

$$C_{loss}^{tot} = k_p \cdot \Delta P_{max} + \int_{t_0}^{t} k_w(\tau) \cdot \Delta P(\tau) d\tau \tag{2.19}$$

$$= k_p \cdot \Delta P_{max} + \Delta P_{max} \cdot k_{w,ekv} \cdot \int_{t_0}^{t} \frac{\Delta P(\tau)}{\Delta P_{max}} d\tau \tag{2.20}$$

$$= (k_p + k_w \cdot \kappa_t) \cdot \Delta P_{max} \tag{2.21}$$

$$= k_{pekv} \cdot \Delta P_{max} \tag{2.22}$$

To calculate k_{pekv}, the specific factors k_p and $k_{w,ekv}$ can be found from the planning guide [43], while κ_t must be calculated or assumed. For the case study, κ_t is calculated. The specific factors depend on the size of the transformer and are stated in section 4.3 for the case study. Almost the same procedure can be done for power line losses.

The power loss costs are important for power grid planning purposes [44]. The annual energy losses in the grid in Norway is about 7.5 TWh, while gross consumption is 137 TWh, which corresponds to 5.4 % [45]. The transformer operational cost consists of copper losses. In case of an investment, that will also be a part of the cost. The calculation of losses are done with equation 2.23.

$$\Delta W = P_k \left(\frac{S}{S_n} \right)^2 \tag{2.23}$$

ΔW - Copper losses [kW]

P_k - Losses at rated power [kW]

S - Transformer load [kVA]

S_n - Transformer rating [kVA]

2.4 Error estimation

By randomly select a data point from a data set to represent the set, bring an error along to the result of running a model, or do a calculation. An error estimate quantifies the deviation from the average value by letting a random data point represent a whole set. By having several runs and calculations with different randomly selected data points, it is possible to calculate an error estimate.

The result from a test run is denominated as C_i (for cost) where i is the index of the test run and $I = \{1, \ldots, N\}$ is the set containing N test runs. Equation 2.24 shows how the

standard deviation is calculated [46].

$$\sigma = \sqrt{\frac{1}{N-1}\sum_{i=1}^{N}(C_i - \bar{C})^2} \cdot 100\% \tag{2.24}$$

where $i = 1, \ldots, N$ and equation 2.25 shows how the average $\bar{C}$ is calculated.

$$\bar{C} = \frac{1}{4}\sum_{i=1}^{N} C_i \tag{2.25}$$

The relative error ε is calculated as a percentage of the standard deviation σ divided by the average result, $\bar{C}$, mathematically shown in equation 2.26.

$$\varepsilon = \frac{\sigma}{\bar{C}} \tag{2.26}$$

The relative error ε indicates the average error of choosing a random data point out of a data set to represent the data set. The more cases (N), which are used to compute the value, increases the significance of the error estimate.

Chapter 3

Method

This chapter builds up the optimization model, which is used to optimize the BESS and its operation. The optimization model needs particular input, such as the load. A method to estimate EV charging demand is presented. In the end, the implementation and a summary will try to make the complete task and method overview clear.

3.1 Assumptions and notations

The BESS is NMC-LMO cell-based, and the size is optimized. The battery degradation must involve several assumptions and linearizations to make it possible to implement and run. The running time quickly increases if the model contains a high order of linearities.

The calender and cyclic aging are separated mathematically. Different impacting variables on the degradation are decoupled, while they, in reality, are coupled and interacting. The degradation mechanisms are, therefore, superpositions of linearized functions. Precalculating the constants reduces the battery energy capacity with time and use.

When the BESS operation is optimized, the charging demand and load are known, which means that there is a perfect forecast when applying the BESS. In reality, this is not possible to predict, and the results from the optimization are in the optimal use of the battery when a perfect forecast of the load and electricity prices are assumed.

There are some sets which describes different time intervals, and they are

- T - set of minutes, where $t \in T$

- H - set of hours, where $h \in H$
- M - set of months, where $m \in M$
- Y - set of years, where $y \in Y$

Δ is used to describe the difference in one variable between time steps to make a more compact notation of recursive variables. For instance, the change in stored energy in the battery $\Delta E_B(t)$ is equivalent with $E_B(t) - E_B(t-1)$. Before the formulation of optimization in detail, the system parameters, economic parameters, and system variables are presented and explained below.

System parameters

P_L	- EV charging demand [kW]
$P_{grid}^{contracted}$	- Maximum grid capacity [kW]
η_c	- BESS charging efficiency [%]
η_d	- BESS discharging efficiency [%]
SoC_{min}	- Minimum level of SoC [%]
SoC_{max}	- Maximum level of SoC [%]
k_t	- Calender ageing factor [1/$\sqrt{\text{min}}$]
$k_{C_{r0}}$	- Cyclic ageing factor constant with respect to C-rate [%/cycle]
$k_{C_{r1}}$	- Cyclic ageing factor linear with respect to C-rate [h %/cycle]
E_{B0}	- BESS energy capacity [kWh]
P_{inv}^{max}	- BESS power capacity [kW]

Economic parameters

c_{spot}	- Spot price [NOK/kWh]
$c_{E,tar}$	- Energy term of the grid tariff cost [NOK/kWh]
$c_{P,tar}$	- Power term of the grid tariff cost [NOK/kW/month]
c_{main}	- Specific battery maintenance cost [NOK/kWh]
$I_B^{E,cap}$	- Specific battery energy investment cost [NOK/kWh]
$I_B^{P,cap}$	- Specific battery power investment cost [NOK/kW]
N	- Number of years [years]
r	- Annually discount rate [%]

System variables

P_{grid}	- Grid power [kW]
P_B	- Battery power [kW]
P_{char}	- Battery charging power [kW]
P_{dchar}	- Battery discharging power [kW]

SoC	- State of charge [%]
FEC	- Full equivalent cycle [cycle]
f_c	- Cyclic ageing factor as function of C-rate [%/cycle]
SoH	- State of health [%]
E_{B0}	- BESS energy capacity [kWh]
P_{inv}^{max}	- BESS power capacity [kW]

Further, the terms calibration model and optimization model are used as names for different setups of the problem. Both describe optimization models but to distinguish between models where the BESS size is a variable and not, to names are applied. The optimization model does not include the BESS size as a variable in the objective function. However, the calibration model has included BESS energy and maximum power as variables in the objective function. The calibration model's purpose is to know the optimal BESS size without including degradation.

3.2 Mathematical formulation for optimization problem

The constraints will be determined in section 3.2.2 and the objective function in section 3.2.1. This section builds up the model to optimize the battery in figure 3.1.

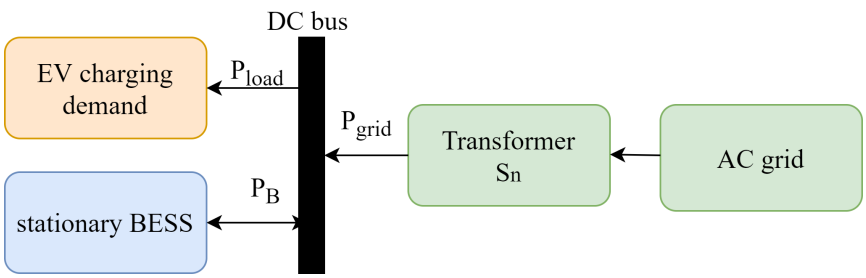

Figure 3.1: FCS and BESS connection.

3.2.1 Objective function

The objective function will be the total costs, which is consisting of several elements. The total cost function C_{tot} reflects the total operational and investment related costs and corresponds to $f(x)$ in section 2.2. There are both operational and investment costs, which for the BESS case are

- spot price for electricity c_{spot}
- grid tariffs, given in energy ($c_{E,tar}$) and power ($c_{P,tar}$) terms

- specific investment costs for BESS for installed energy and power capacity, $I_B^{E,cap}$ and $I_B^{P,cap}$

The customer pays the electricity price and energy tariff for each unit of energy imported from the grid. The power tariff is paid based on the maximum grid power during each month. The specific cost marked with P, cap is proportional to the maximum battery power, while the cost marked with E, cap is proportional to the installed energy capacity.

Instead of having a cost element in the objective function, reflecting the cost of battery degradation, SoH reflects the degradation, which represents energy storage capacity. Based on the presented model in section 2.1, the operational constraints includes battery degradation. Battery degradation leads to higher power tariff costs due to the BESS's reduced ability to peak shave because of the reduced capacity due to degradation. The discounting factor α, presented in section 2.3, is incorporated on yearly basis. The grid tariffs are a monthly based fee, and therefore monthly time steps must be incorporated. The variables have a time step interval in minutes. The smallest time step is minutes, while hours are the longest lasting time step, such as the spot prices, which are hourly changing. For notation simplicity, by applying equation 3.1, minute-based power is transferred to hour-based, which leads to the grid energy for one hour.

$$E_{grid}(h) = \sum_{t=1}^{60} P_{grid}(t)\Delta t \tag{3.1}$$

The objective function is the sum of the costs. For the calibration model, the costs of the BESS investment must be included to be minimized. The BESS size is set and only operational variabels are optimized in the optimization model. These variabels includes power for the BESS and grid as well as the degradation of the BESS. Ideally, the BESS size would be part of the cost function, and the model would give the optimal case. Due to limited computer power, this is not possible due to too high non-linearities in the degradation constraints. This is the reason why the BESS size will be omitted in the optimization model and pres-set from the calibration model. The objective function for the calibration model is

$$C_{cal,tot} = \sum_{y \in Y} \alpha(y) \Big[\sum_{m \in M} c_{P,tar}(m) \cdot P_{grid}^{max}(m) + \sum_{h \in H} E_{grid}(h) \Big(c_{spot}(h) + c_{E,tar}(m) \Big) \Big] + I_B^{E,cap} \cdot E_{B0} + I_B^{P,cap} \cdot P_{B,max} \tag{3.2}$$

and for the optimization model

$$C_{opt,tot} = \sum_{y \in Y} \alpha(y) \Big[\sum_{m \in M} c_{P,tar}(m) \cdot P_{grid}^{max}(m) + \sum_{h \in H} E_{grid}(h) \Big(c_{spot}(h) + c_{E,tar}(m) \Big) \Big] \quad (3.3)$$

Objective function 3.2 is including the BESS size. By adding constraints to the problem, and then minimize function 3.2, the result will be the optimal size of the BESS, the maximum grid power each month, and the minimum costs.

3.2.2 Constraints

The BESS operation and its degradation mechanisms must be formulated mathematically as constraints. The constraints set the boundaries of the feasible region in the overall optimization formulation. An overview of a situation with an EV FCS integrated with a BESS is in figure 3.1. The power balance at the DC bus must be satisfied at all times $t \in T$ and ensured by the first constraint:

$$P_{grid}(t) + P_B(t) = P_{load}(t) \quad (3.4)$$

as seen in figure 3.1. When the battery is charging, P_B is negative and more power is drawn from the grid than just the load. The connected transformer has a rated power S_n as shown in figure 3.1 which determines the limit of the grid power. The FCS operator has a contracted capacity, $P_{grid}^{contract}$, corresponding to S_n, with the DSO, which gives:

$$P_{grid}(t) \leq P_{grid}^{contract} \quad (3.5)$$

The battery variables SoC and SoH are defined with equation 2.1, 2.2, 2.3 and 2.4 as in section 2.1.2. The power which the BESS can provide is limited by the nominal power of the inverter, P_{inv}^{max}. These characteristics are incorporated in the following constraints which can be added to the cost minimization problem:

$$P_{char}(t) \leq P_{inv}^{max} \tag{3.6}$$

$$P_{dchar}(t) \leq P_{inv}^{max} \tag{3.7}$$

The variable E_B is the amount of energy which is stored in the BESS and must be updated every time step. The maximum energy charged and discharged are based on the BESS' capacity $E_{B,cap}$ and the SoC limits. E_B is limited by the SoC limits stated in constraint 2.3 and 2.4. There is an energy loss while charging and discharging the battery, and that is reflected in the charigng and discharging efficiences, η_c and η_d. The energy balance in the BESS is mathematically [11]:

$$E_B(t) = E_B(t-1) + \eta_c \cdot P_{char}(t)\Delta t - \eta_d \cdot P_{dchar}(t)\Delta t \tag{3.8}$$

Assuming that the efficiencies are below one, equation 3.8 will make sure that the discharging and charging power is not simultaneously different from zero. The definition of battery power, P_B is the difference between the charging and discharging power. When the battery is charging, the grid power is higher than the load power, which means that the battery power is negative according to equation 3.4. Thus, battery power is:

$$P_B(t) = P_{dchar}(t) - P_{char}(t) \tag{3.9}$$

As mentioned in the problem description in section 1.2, degradation of the BESS is included in the optimization. The SoH will be the measure of degradation, and at all times available energy storage capacity E_B is SoH times the initial energy storage capacity E_{B0}. The constraints is as defined in equation 2.1.

The SoH depends on several factors, temperature T_K, time t, C-rate C_r and FEC. C_r and FEC are defined in respectively equation 2.8 and 2.7. Some of these degradation-driving factors will be set constant values, while others will be variables. Ideally all of them are a variable. The temperature is assumed to be constant, maintained by the battery managament system (BMS). The FEC is the eqvivalent amount of cycles the BESS has experienced and the sum of all SoC changes through the entire BESS life. The Wang model presented in section 2.1.2 suggests that SoH decreases the available energy capacity as a function linear proportional to the squareroot of time and linear proportional to FEC.

The Wang model is applied and recognized as a well-suited model for capturing battery degradation [3]. Equation 2.12 in section 2.1.2 calculates the lost capacity based on the Wang model [26] and is defining the negative terms in the SoH function, formulated as:

$$SoH(t) = SoH(t_0) - k_t(T_K) \cdot \sqrt{t} - f_c(T_K, C_r) \cdot FEC(t) \tag{3.10}$$

If the temperature T_K is given, only the last term in equation 3.10 is non-linear. The multiplication factor f_c is corresponding to the factor $(a \cdot T_K^2 + b \cdot T_K + c)e^{(d \cdot T_K + e) \cdot C_r(t)}$ given in equation 2.12 according to the Wang model [26]. The exponent $(d \cdot T_K + e) \cdot C_r$ is where the C-rate is included. Appendix B calculates the approximation of the exponential term. By setting the temperature T_K to a constant T_0, the final function $f_c(T_0, C_r(t))$ is:

$$f_c(T_0, C_r) = k_{C_r 0} + k_{C_r 1} \cdot C_r(t) \tag{3.11}$$

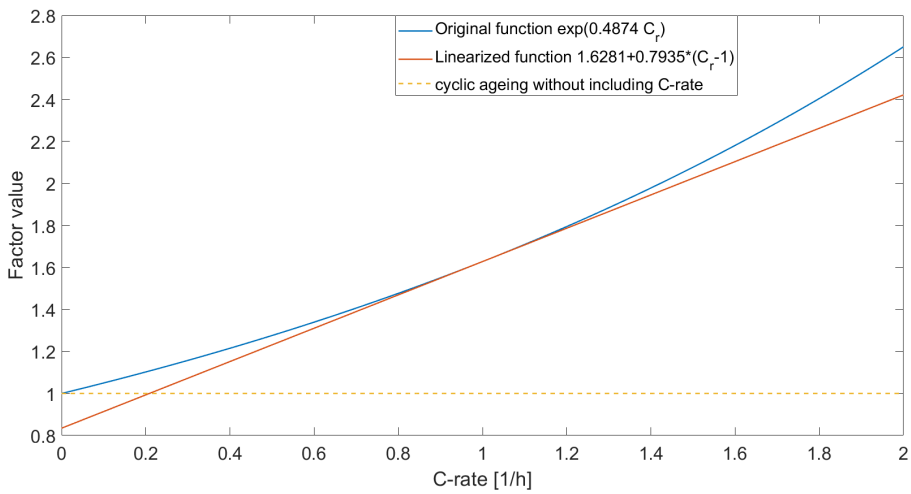

Figure 3.2: Exponential function (original function), the linearized function and the case of not including C-rate.

In figure 3.2, the blue line is the ideal impact of C-rate. The red line is the linear approximation, and the yellow dashed line is if the C-rate is assumed to be one, and thus make f_c a constant. The constraints of SoH would be linear in that case. The linearized function underestimates the C-rate below one and overestimates it above one. Compared to assuming a constant C-rate of 1, the linearized version is closer to the ideal case. The

term which will represent the cyclic aging of the battery will be quadratic because of the multiplication of the linear variables f_c and FEC.

3.2.3 Problem formulation

As stated in section 3.2.1, the optimization problem has a objective function and several operational constraints, which can be equalities and inequalites. The objective function is the investment costs and operational costs for the FCS operator and the objective function is derived in section 3.2.1. The constraints are derived in section 3.2.2 and section 2.1.2. The inequality constraints include limitations on variables while the equality constraints forces the battery operation and degradation to satisfy the physical conditions. All the constraints are now summarized in this section in the finite definition of the optimization problem. To estimate the optimal BESS size, a linear optimization model without degradation constraints, referred to as the calibration model, is defined as:

$$\underset{\substack{P_{grid}^{max},\\ P_B^{max},E_{B0}}}{\text{minimize}} \quad \sum_{y\in Y}\alpha(y)\Big[\sum_{h\in H}E_{grid}(h)\Big(c_{spot}(h)+c_{E,tar}(m)\Big)+\sum_{m\in M}c_{P,tar}(m)\cdot P_{grid}^{max}(m)\Big]+I_B^{E,cap}\cdot E_{B0}+I_B^{P,cap}\cdot P_{B,max} \tag{3.12a}$$

$$\text{subject to} \quad P_L(t)=P_{grid}(t)+P_B(t) \qquad \forall t\in T \tag{3.12b}$$

$$P_B(t)=P_{dchar}(t)-P_{char}(t) \qquad \forall t\in T \tag{3.12c}$$

$$\Delta E_B(t)=\eta_c\cdot P_{char}(t)\Delta t-\frac{1}{\eta_d}\cdot P_{dchar}(t)\Delta t \qquad \forall t\in T \tag{3.12d}$$

$$SoC(t)=\frac{E_B(t)}{E_{B0}} \qquad \forall t\in T \tag{3.12e}$$

$$P_{char}(t)\leq P_{inv}^{max} \qquad \forall t\in T \tag{3.12f}$$

$$P_{dischar}(t)\leq P_{inv}^{max} \qquad \forall t\in T \tag{3.12g}$$

$$SoC(t)\geq SoC_{min} \qquad \forall t\in T \tag{3.12h}$$

$$SoC(t)\leq SoC_{max} \qquad \forall t\in T \tag{3.12i}$$

$$P_{grid}(t)\leq P_{grid}^{contract} \qquad \forall t\in T \tag{3.12j}$$

To find the optimal BESS configuration for the case study, several selected BESS size configurations based on the result from the linear optimization above. The optimization model, referred to as the optimization model, is:

$$\underset{P_{grid}^{max}}{\text{minimize}} \quad C_{tot} = \sum_{y \in Y} \alpha(y) \Big[\sum_{h \in H} E_{grid}(h) \Big(c_{spot}(h) + c_{E,tar}(m) \Big) + \sum_{m \in M} c_{P,tar}(m) \cdot P_{grid}^{max}(m) \Big] \tag{3.13a}$$

subject to

$$P_L(t) = P_{grid}(t) + P_B(t) \qquad \forall t \in T \tag{3.13b}$$

$$P_B(t) = P_{dchar}(t) - P_{char}(t) \qquad \forall t \in T \tag{3.13c}$$

$$\Delta E_B(t) = \eta_c \cdot P_{char}(t)\Delta t - \frac{1}{\eta_d} \cdot P_{dchar}(t)\Delta t \qquad \forall t \in T \tag{3.13d}$$

$$E_{B,cap} = SoH(t) \cdot E_{B0} \qquad \forall t \in T \tag{3.13e}$$

$$SoC(t) = \frac{E_B(t)}{E_{B,cap}} \qquad \forall t \in T \tag{3.13f}$$

$$C_r(t) = \frac{P_B(t)}{E_{B0}} \qquad \forall t \in T \tag{3.13g}$$

$$SoH(t) = SoH(t_0) - k_t \cdot \sqrt{t} - f_c(t) \cdot FEC(t) \qquad \forall t \in T \tag{3.13h}$$

$$\Delta FEC(t) = \frac{1}{2} \cdot \frac{P_{char}(t) + P_{dchar}(t)}{E_{B0} \cdot (SoC_{max} - SoC_{min})} \Delta t \qquad \forall t \in T \tag{3.13i}$$

$$f_c(t) = k_{C_r 0} + k_{C_r 1} \cdot C_r(t) \qquad \forall t \in T \tag{3.13j}$$

$$P_{char}(t) \leq P_{inv}^{max} \qquad \forall t \in T \tag{3.13k}$$

$$P_{dischar}(t) \leq P_{inv}^{max} \qquad \forall t \in T \tag{3.13l}$$

$$SoC(t) \geq SoC_{min} \qquad \forall t \in T \tag{3.13m}$$

$$SoC(t) \leq SoC_{max} \qquad \forall t \in T \tag{3.13n}$$

$$P_{grid}(t) \leq P_{grid}^{contract} \qquad \forall t \in T \tag{3.13o}$$

3.3 EV charging demand estimation method

This section describes the method to estimate the EV charging demand in figure 3.1. A method is necessary, when the only information is the number of chargers and the maximum power of the chargers, to estimate the EV charging demand. The method used to determine the charging demand builds on a technique developed during the author's work on a specialization project during fall 2019 [13]. Appendix A contains more details for the theoretical build-up of the method developed in the project. The appendix explains the stochastic behavior and connections between the arrival time, inter-arrival time, and the number of cars arriving each hour. Their expectation values are based on a large scale

data set for EV charging (excluded home charging) for one year for whole Norway. That does include not only FCSs but also single/multiple ordinary public charging points. Some adjustments are made to be able to estimate the EV charging demand based on the given information.

The interarrival-time, charging time, and EV type of every arriving car are given from probability functions and user-set input. The necessary input to estimate EV charging demand is

- number of arriving cars each day
- number of chargers and its rated power
- EV distribution

The EV distribution is constant and based on today's composition of the EVs in Norway. Table 3.1 shows the fractions of the top 10 EV models in Norway on December 31st, 2019. This is the basis for the distribution of EVs used in the charging demand estimation.

Another input that must be decided upon by the user is the average total amount of cars that arrive at the FCS every day. In addition to the number of chargers at the FCS.

Table 3.1: Key figures for modeling of EV charging demand at FCS.

EV model	Number of EVs	Fraction of top 10 [%]	Battery size [kWh]	DC power charging [kW]	Driving range winter/summer [km]
Nissan Leaf	55 964	26.4	30	50	125/190
Volkswagen e-Golf	39 608	18.7	35.8	40	200/300
BMW i3	23 951	11.3	42	50	200/275
Tesla model S	19 876	9.4	98.5	120	400/550
Kia Soul	16 899	8.0	31.8	80	150/220
Tesla model 3	13 593	6.4	80	150	400
Tesla model X	12 793	6.0	98	120	350/380
Renault ZOE	11 492	5.4	41	22	300
Volkswagen e-Up!	9 438	4.5	18.7	40	120/165
Hyuandai IONIQ	8 331	3.9	30.5	70	160/240
Sum	211 945	100			

The time step in the EV charging demand estimation method is in minutes. If the time resolution for optimizing is hours, hours are the smallest time step, thus charging demand is in hours. The hourly demand is calculated by computing an average value for each hour from the charging demand in minutes, mathematically done by equation 3.14 for each hour h.

$$P_L^h(h) = \frac{1}{60} \sum_{t=1}^{60} P_L\Big(t + 60 \cdot (h-1)\Big) \qquad \forall h \in H \tag{3.14}$$

$P_L^h(h)$ - hourly EV charging demand [kW]

$P_L(t)$ - original EV charging demand in minutes [kW]

3.4 Implementation and solvers

To implement the optimization problems in 3.2.3, Ipopt in Julia is used as a solver. Visual Studio Code is used as a platform to write code and compiling the code. Ipopt is an interior point algorithm implemented to solve nonlinear optimization problems, and the constraints can be both convex and non-convex. Appendix C shows the mathematical method of the interior point method.

The advantage of using Julia to do the optimization is the JuMP package, which is a userfriendly optimization tool. Julia is a programming language developed at MIT with high-level syntax and low level running time [47]. For the sake of consistency, Matlab is used to make the plots. The implementation of the EV charging demand estimation method is in Matlab. Figure 3.3 gives an overview of the application and connection between the input and models.

Figure 3.3 shows the overall build-up of the method in this thesis. The modeling of the EV charging demand and the processing of selecting a day to represent the month is done in Matlab. The EV charging demand is exported to Julia as part of the input to the optimization. After the optimization is done in Julia, the results are exported back to Matlab, and the results are then processed in Matlab as well. As seen in figure 3.3, the optimization formulation, which is build up and stated earlier in this chapter, need an input. The input can be every relevant load each individual wants to look at, and in this thesis, it is an EV FCS in Trøndelag, Norway. The EV charging demand at the FCS, which is the input to the calibration and optimization model, is the topic of the next chapter.

The representation of a month with one day makes the implementation not entirely straight

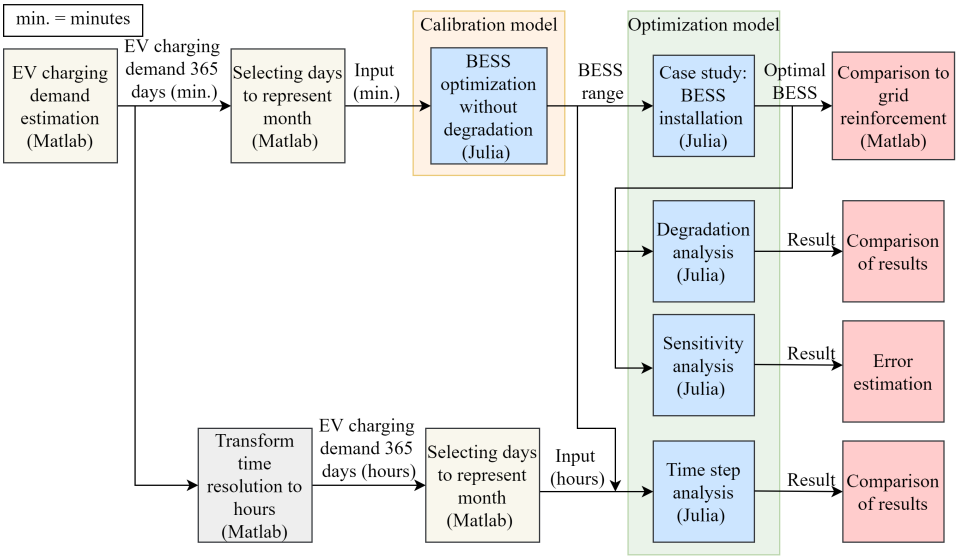

Figure 3.3: Overview of data selection and application of the optimization model.

forward. The variables and most of the constraints are the same, except SoH. When FEC is calculated, every change is multiplied with the number of days in that month. The reason is that the same day will go over again for such many times. Also, this is taken care of in the square root of time function describing calender aging. The same applies to the objective function, where costs that are repeated every day of a month. The cost element and the number of days are multiplied. The implementational technicalities are not described in the formulation of the optimization model. This representation is done for reasons regarding computational power available. Appendix D states the complete and detailed formulation, which is implemented incorporating the daily representation of a month mathematically.

Chapter 4

Case study

This chapter presents the case study in section 4.1. Section 4.2 presents the results from modeling the EV charging demand for three cases. The first case is today's situation, the second is a situation if the number of chargers increases with 50 %, and the third is if the time step is in hours instead of minutes. The EV charging demand is the fundament of establishing a case where the EV charging demand is input to the optimization model. The numeric parameter values for the case study are summarized in section 4.3.

By including quadratic constraints about battery degradation, the computational effort to solve a massive problem is increasing massively with the number of equations and variables [48]. It is not easy to avoid it when degradation is in the operational constraints and described by a SoH variable. An EV charging demand on a minute time basis as input to an optimization problem has a too large RAM need to run on a computer with 64-bit Windows 10, Intel® Core™ i5-8250U 1.80GHz CPU and 8 GB of RAM. That is the reason behind the choice of having one day represent one month, which will be repeated and underlined in this chapter. The idea is to reduce the necessary computational effort, such that the optimization model can run for a more extended period.

4.1 Introduction to case study

A DSO regularly experiences that the load (power and energy demand) is changing. The DSO is responsible for delivering enough power and energy for all consumers at all times. The traditional approach to meet a load increase is to reinforce the grid. An alternative to this is applying BESS. However, the DSO has strict restrictions to operate a BESS itself

[41]. The consumers can, however, install and operate BESS, and that is the second option to meet a load increase.

A load increase or power demand increase is the reason for conducting a case study to apply BESS for peak shaving purposes. During a specialization project in the fall 2019, the EV charging demand at an EV FCS was estimated with a particular method presented in section 3.3 with more detailed description in appendix A. This charging demand was generated for one year with a resolution on a minute basis.

The case study is for an EV FCS in Trøndelag based on real data. Today's EV charging demand is shown in figure 4.2. If the FCS operator installs 50 % more chargers, the EV charging demand is as shown in figure 4.4. The EV charging demand in the case study is from figure 4.4. It is from now on an input to the calibration and optimization models.

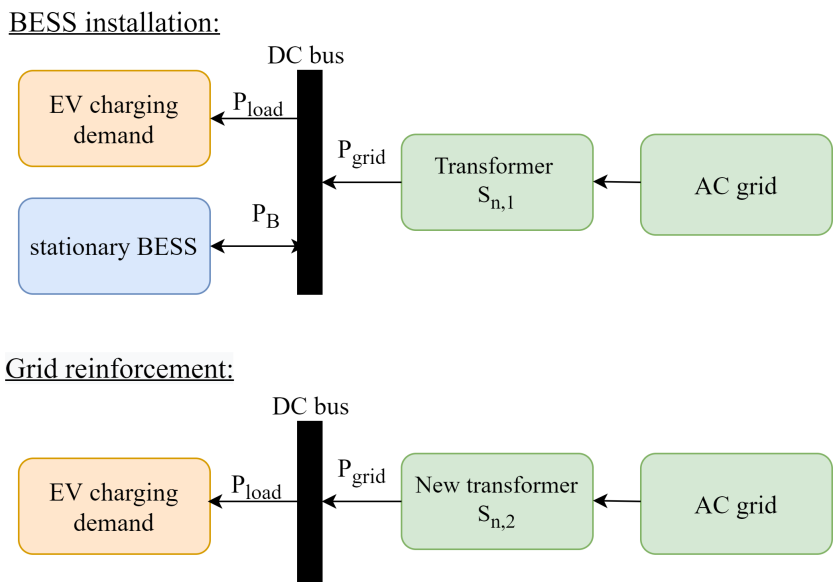

Figure 4.1: Overview of case study.

The two options to meet the increased EV charging demand are:

1) grid reinforcement

2) install BESS to peak shave

To avoid to violate the contracted power of 1250 kVA, denoted $S_{n,1}$ in figure 4.1, the FCS must install a BESS. The FCS operator makes the investment costs regarding the BESS. If the FCS operator does not invest in a BESS, the increase of EV charging demand due to the increase of 50 % more available chargers, force it to invest in a new transformer at

the substation. The necessary transformer is dimensioned to 1600 kVA, denoted $S_{n,2}$ in figure 4.1.

The case study consists of two calculations, one for grid reinforcement and one for the use of an optimal BESS. Figure 4.1 shows an overview of the two considered options of the case study. Section 2.3 provides NPV assessment method.

4.2 Results from EV charging demand modeling

Today, the EV FCS consists of two 22 kW chargers, two 50 kW chargers, and twelve 150 kW chargers. The agreed capacity is 1250 kW.

Table 4.1: Clustered EV groups with key figures. This is the input to the EV charging demand estimation method.

Group	Fraction [%]	Battery size [kWh]	DC charging power [kW]
a	5.4	41	22
b	60.9	33.2	50
c	33.7	71.2	150

For the EV charging demand method, the EV composition of Norway's top ten EVs in table 3.1 is clustered into three groups. EVs with charging power of 22 kW or less merges into group a. EVs with charging power equal to or less than 50 kW and higher than 22 kW merges into group b. The rest, EVs with a charging power higher than 50 kW merges into group c. The clustered groups are a uniform distribution and are the distribution used as input in the model to generate the EV charging demand at the FCS. Table 4.1 shows the distribution of EVs.

The EV charging demand in the case is the estimated charging demand if the FCS increases the number of chargers with 50 %. That means that the FCS will have three 22 kW chargers, three 50 kW chargers, and eighteen 150 kW chargers. The 150 kW chargers are in pairs and regulated to have a power of 150 kW in total for each pair. The aggregated maximum power today with twelve 150 kW chargers is then 150 kW times 6, which is 900 kW. The total theoretical power peak is the sum of all 900 kW and the four others, which gives a total of 1044 kW. Thus, today's theoretical maximum power is less than the contracted power of 1250 kW. With a 50 % increase, the total theoretical peak power is 1566 kW, and 1250 kW will not be enough. If the FCS operator installs a BESS, it must cover at least 316 kW to keep the agreement of a maximum power of 1250 kW.

Ten independent charging demands make an average profile. Matlab decides which of the then charging demands that correlates best with the average. That profile is the resulting EV charging demand. Finally, note that the method to estimate EV charging demand does not distinguish between weekdays and weekends.

4.2.1 EV charging demand today

As mentioned, the EV FCS consists of two 22 kW chargers, two 50 kW chargers, and twelve 150 kW chargers and has an agreed capacity of 1250 kW today. Table 4.1 is input to the EV charging demand estimation algorithm, and as well as average cars per day, which is 250 for today's situation.

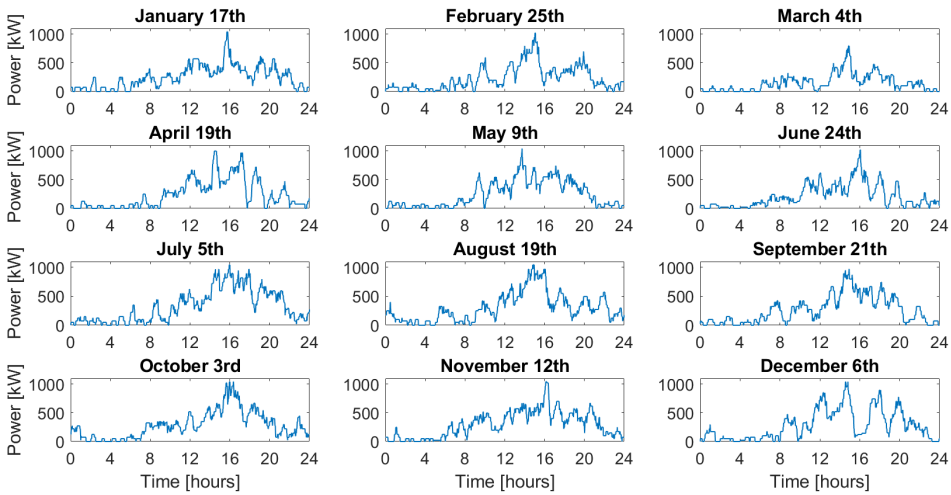

Figure 4.2: EV charging demand for the selected days that represent their month in todays situation. The selection criterion in each month is the highest daily peak power.

The EV charging demand has a resolution of minutes, and the power and energy balance will be on a minute basis. Thus, the degradation mechanisms depend on this, and the non-linear constraints are on a minute basis. Two possible measures can make it possible to run an analysis for several years. Either the time step can increase to hourly intervals or each month can have one representative day, which will be in the optimization on a minute basis. The latter method is applied where each month is represented by one day, to capture the degradation on a minute basis. The criterion for the selection of each month's representative day is peak power. For January, the day with the highest power peak is representing January, and so on. By making this selection, figure 4.2 shows the days used to describe the whole year in the optimization.

Figure 4.3 shows January as a visual example of the selection of days. The figure shows

plots of every day in January, and the day with the highest power peak is bold black.

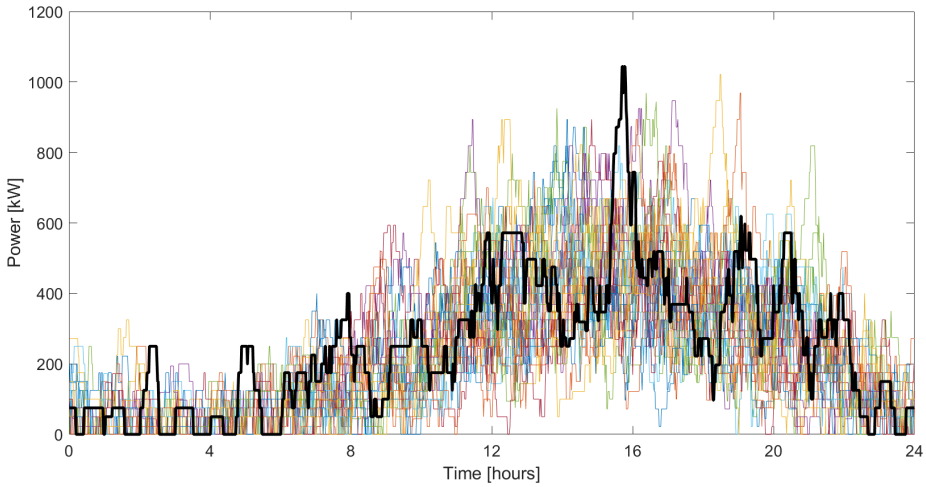

Figure 4.3: Visual example from January on the selection of days to represent the month in today's situation. It is all days in January where the selected day in bold black.

4.2.2 EV charging demand for increased number of chargers

The case study is based on that the operator decides to increase the number of chargers with 50 %. Then the FCS will have three 22 kW chargers, three 50 kW chargers, and eighteen 150 kW chargers. The EV charging demand generated is in minutes, and the same applies to the case formulation as for today's situation. One day will represent each month, and the day with the highest power peak will be chosen. By making this selection, figure 4.4 shows the days which represent a whole year in the optimization.

Figure 4.5 shows January as a visual example of the selection of days. The figure shows the plot of every day in January, and the day with the highest power peak is bold black. The day in bold black is, therefore, also the selected day for January. The concept of one day representing one month will initiate the need to select spot prices to represent each month, and this is done in subsection 4.3. The spot prices will not necessarily be the same day as the EV charging demand. There is no reason to pick the same date because the EV charging demand is randomly generated and not connected to particular days in reality.

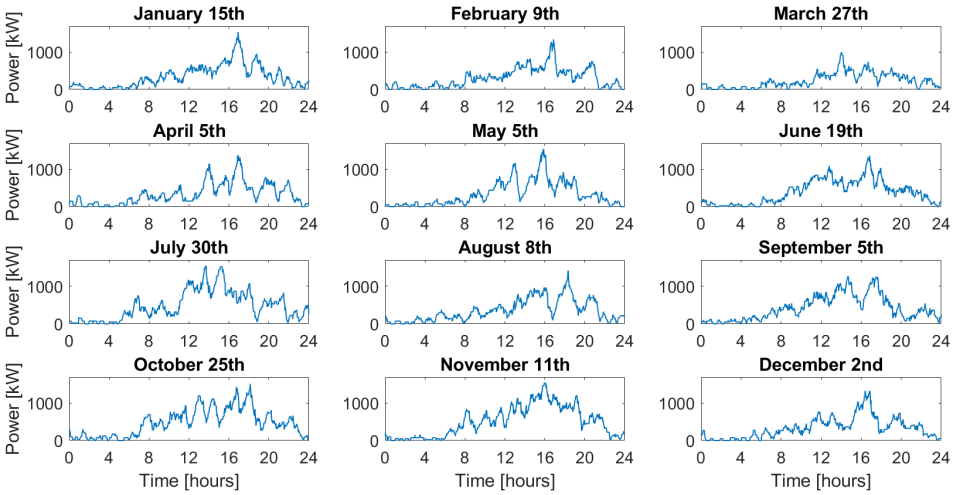

Figure 4.4: EV charging demand for the selected days that represent their month for the case study. The selection criterion in each month is the highest daily peak power.

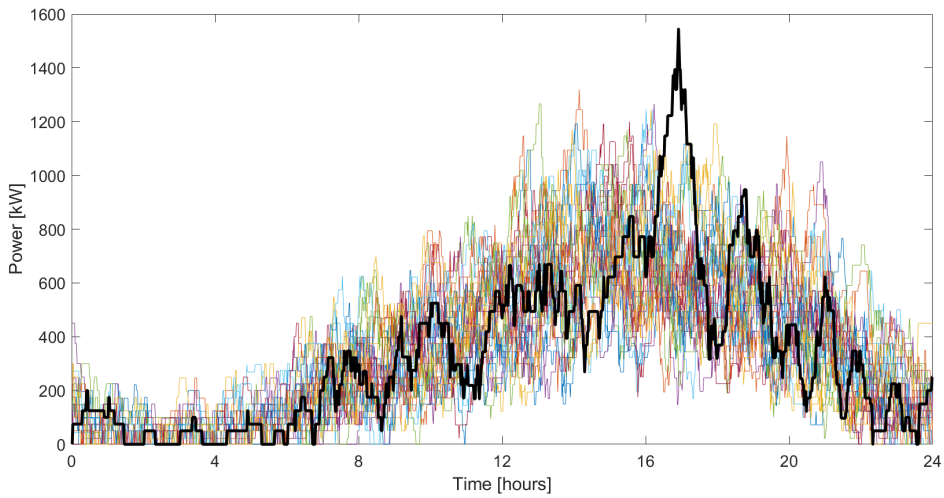

Figure 4.5: Visual example from January on the selection of days to represent the month for the case study. It is all days in January where the selected day in bold black.

Table 4.2 shows some describing figures for the EV charging demand. E_{rep} is the energy of the selected day for that month multiplied with the number of days. E_{est} is the total EV charging energy demand for the month in the original EV charging demand before the selection of a day.

Table 4.2: Monthly energy consumption (after the selection of days representing one month) at FCS for the case study (E_{rep}) compared to the estimated EV charging demand (E_{est}).

Month	Days	E_{rep} [MWh]	Percent of total [%]	E_{est} [MWh]	Δ [MWh]
January	31	253.38	7.7	256.81	-3.43
February	28	205.65	6.2	212.04	-6.39
March	31	176.36	5.4	174.77	1.59
April	30	239.67	7.3	228.56	11.11
May	31	252.44	7.7	237.45	14.99
June	30	282.13	8.6	256.80	25.33
July	31	357.40	10.9	327.47	29.93
August	31	261.20	7.9	276.27	-15.07
September	30	299.98	9.1	270.80	29.18
October	31	353.85	10.7	339.14	14.71
November	30	363.77	11.0	306.91	56.86
December	31	246.26	7.5	273.36	-27.10
Total one year	365	3 292.08	100	3 160.38	131.70

In the optimization with this EV charging demand as input, the desired goal is to get an optimal BESS based on NMC-LMO cells. The BESS has the same characteristics as in the original experiments of the Wang model [26]. Compared to other lithium-ion batteries, the NMC-LMO variant has a good overall performance considering factors as energy density, cost, life span, safety, and specific energy [49]. The degradation constants are calculated in section 3.2.2 based on constants for the model in table 2.3. The presence of LMO will accelerate the SEI growth and thus calender aging [26]. The Wang model for degradation is giving a relatively fast degradation compared to other models [21].

To sum up, the input to the optimization problem, the EV charging demand, is twelve days, representing one year. Each day represents their month, selected with the criterion of highest daily peak power. The days were picked out from a modeled EV charging demand for 365 days based on information about the particular FCS in Trøndelag and stochastical data. The reason for selecting one day to represent one month is for computational purposes. The reason for having a minute resolution is to capture the degradation within a small time frame. For all analyses and results, the twelve days will be input to the

optimization.

4.2.3 Time step transformation

The time step can now be transformed from minutes to hours by applying equation 3.14. This subsection shows the resulting EV charging demand for the case of converting the time step from minutes to hours, and then select the days to represent the month by picking the days with power peaks. The EV charging demand with the hourly resolution is only used for comparison to minute resolution. All other degradation and sensitivity analysis with EV charging demand are in minutes, not in hours.

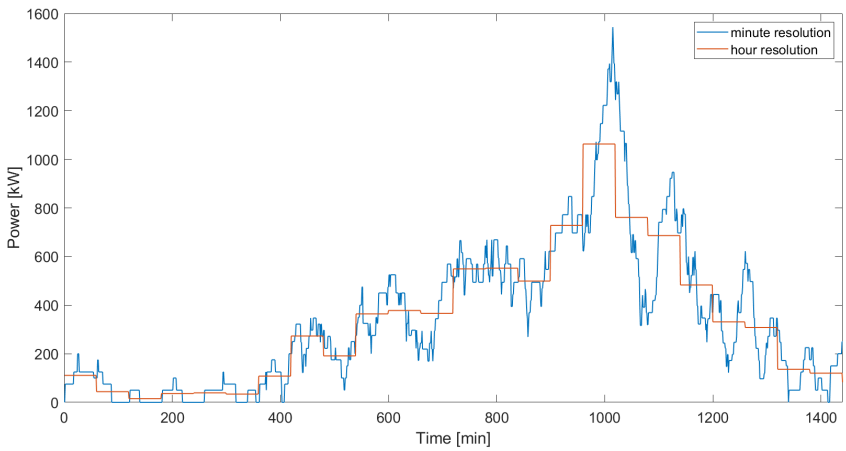

Figure 4.6: The selected day in January as example for EV charging demand at FCS with minute and hourly resolutions (January 15th). The blue graph is with minute resolution and the red is with hourly resolution.

The blue graph in figure 4.6 shows the day representing January in the case study presented in subsection 4.2.2. The red graph is the aggregated EV charging demand with a time resolution in hours. The blue graph is the same as in figure 4.4 and is the first output from the modeled EV charging demand. The main observations from this example are the reduced peak power and smoothening of rapid variations. The peak during the day, which represents January, reduces from 1544 kW to 1063 kW with the transformation of resolution from minutes to hours. The reduction of daily peaks will be the case of every day because the average cannot be higher than the highest single value used to calculate the average. If the day with hourly resolution and minute resolution is the same, the total amount of energy is the same, but the power peaks are different.

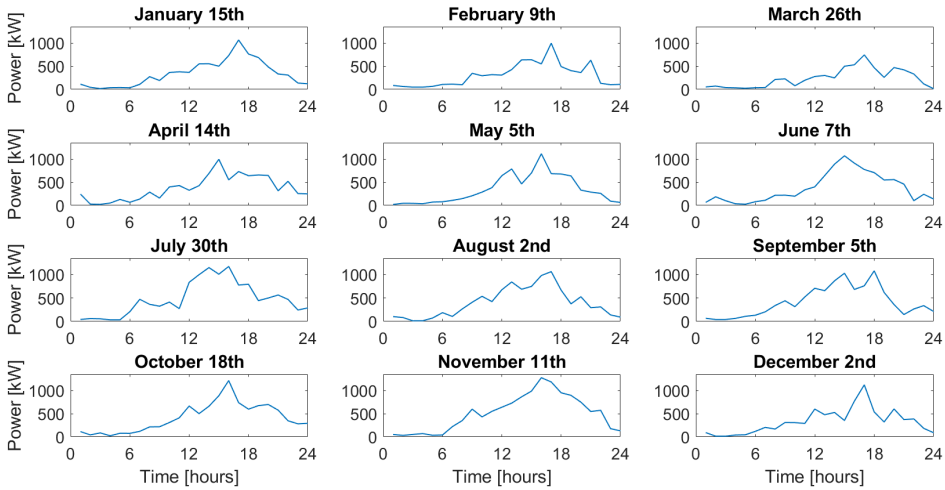

Figure 4.7: EV charging demand for the selected days that represent their month for the case study after the time step transformation. The selection criterion in each month is the highest daily peak power.

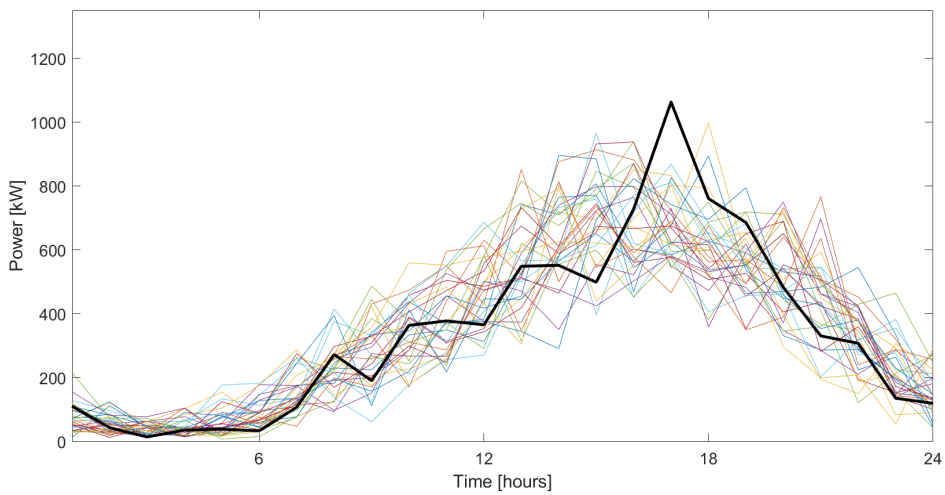

Figure 4.8: Visual example from January on the selection of days to represent the month with hourly time resolution. It is all days in January where the selected day in bold black.

Figure 4.7 shows the selected days when the time step is hours. The selection happens *after* the transformation of the EV charging demand for the whole year from minutes. The days selected are for most months different compared to the selected days in the case study.

Figure 4.8 shows all the 31 days in January with an hourly time resolution. The power

profile in bold black is the day with the highest peak power and is, therefore, the selected day to represent the month. For January, it is coincidentally the same, but that is not the case for the rest of the months.

Figure 4.9 shows the maximum power from the EV charging demand with resolution in minutes and hours for the charging demand. When the resolution is in minutes, the lowest value is 997 kW in March, and the highest is 1544 kW in January, May, July, and November. For a resolution in hours, the lowest value is 742 kW in March, and the highest is 1275 kW in November.

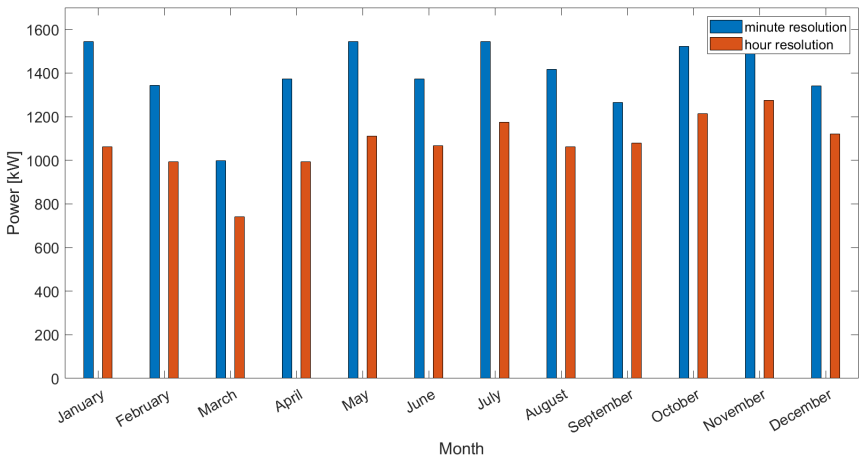

Figure 4.9: Monthly maximum power at EV FCS with resolution in minutes and hours. The blue bars are with minute resolution and the red bars are with hourly resolution.

4.3 System parameters

The price for electricity used in the analysis in this Master's thesis is the historic set of hourly spot prices from 2019. Nordpool's website provides downloadable data. Each month is represented by one chosen day. Therefore a particular day with spot prices must be selected to represent the month. The EV charging demand does not distinguish between weekends and weekdays. The day which will represent the spot prices each month will be picked randomly from all the weekdays each month. Section 5.3.1 contains the results from a sensitivity analysis and an estimate for uncertainty by randomly select a day to represent the month based on a method presented in subsection 2.4. Figure 4.10 shows the price used in the case study, randomly picked from the historical spot prices from 2019.

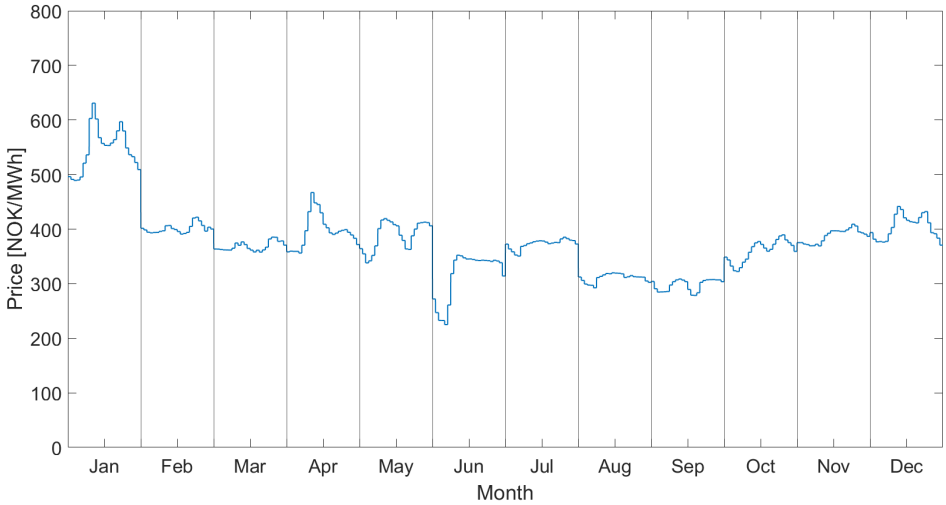

Figure 4.10: Spot prices from 2019 randomly selected and applied in the analysis of the case study.

The regulator, NVE, set the layout of the tariffs for using the grid. The DSOs adjust the level of the costs according to their needs. Since the EV FCS is in Trøndelag, grid tariffs from that region are used in the case study. Table 4.3 contains the grid tariffs from Tensio.

Table 4.3: Grid tariffs today in Trøndelag [39].

	Fixed fee [NOK/year]	Energy tariff [NOK/MWh]	Power tariff [NOK/kW/month]
LV: October - April	8818	65.1	81.6
LV: May - September	8818	65.1	0
HV: October - April	15512	44.5	73.6
HV: May - September	15512	44.5	0

Table 4.4 sums up all the parameters used in the optimization model for the case study. Limitations for SoC is set to a minimum value of 20 % and a maximum value of 90 % to reduce degradation. The voltage is approximately linear to SoC in that region [50], and the degradation models fit best in this region.

The residual value of a BESS is assumed to be 25 % of its initial value when SoH is 80 %. The reason is that the considered EoL can be lower than 80 % for BESS.

For a 1600 kVA transformer, the value of the losses at rated power, P_k, is 13.1 kW, according to Wahl Gundersen Master's thesis [44]. For a 1250 kVA transformer, the value of P_k is 9.7 kW. Based on the losses ΔW, the utilization time of losses, κ_t, is calculated for the case when no BESS is installed, when the rated power transformer is 1600 kVA, and also when the BESS is installed, when the rated power transformer is 1250 kVA.

According to the planning guide from SINTEF Energy [43] the transformer specific loss cost factors with 2020 price level are

- $k_p = 585$ NOK/kW/year
- $k_w = 0.261$ NOK/kWh/year

The nominal power of the inverter, P_{inv}^{max}, as well as the initial battery energy storage capacity, E_{B0}, is being varied between respectively 300 and 400 kW, and 225 and 350 kWh. After the optimization for the BESS sizes and configurations, the optimization model will give a result with minimum total costs. For power tariff sensitivity, the same BESS range is used to see how the cost function is affected. For the rest of the sensitivity analysis, the optimal BESS configuration based on the case study is applied.

The temperature is assumed to be managed by the BMS to lay around 5°C for all $\forall t \in T$. Thus, the temperature will be set to 5° C = 278 K and is fundamental to calculate the constants. One of the optimization tasks of the BMS is to maximize performance and lifetime by limiting temperature deviations [51].

For battery degradation, several constants muse be determined. The constants k_t and k_c in constraint 3.13h must be determined. Section 2.1.2 provides several approaches and ways to calculate som constants. The k_t is the time based constant and determines the pace of calender ageing. The capacity decrease is proportional to the squareroot of time according to all the presented models in section 2.1.2. Using the values for the given constants in table 2.3, T_K = 5°C, the constant $k_t = 0.3706\ \%/\sqrt{\text{day}}$ where the % is the decrease of SoH value. The constant $k_{C_{r0}}$ and $k_{C_{r1}}$ that scales the FEC including C-rate are $1.903 \cdot 10^{-3}$ %/cycle and $1.809 \cdot 10^{-3}$ %/cycle. The temperature dependent constant in the cyclic degradation term is included in $k_{C_{r0}}$ and $k_{C_{r1}}$. Detailed calculation for the linearization constants is shown in appendix B as mentioned in section 3.2.2.

Table 4.4: Applied numeric values for the parameters in the optimization model for the case study.

Parameter values		
Parameters	Unit	Value
$c_{P,tar}$	NOK/kW/month	Table 4.3 (LV)
$c_{E,tar}$	NOK/kWh	Table 4.3 (LV)
c_{spot}	NOK/kWh	Figure 4.10
$I_B^{E,cap}$	NOK/kWh	1700
$I_B^{P,cap}$	NOK/kW	5525
$P_{grid}^{contract}$	kW	1250
E_{B0}	kWh	determined from the calibration model result
P_{inv}^{max}	kW	determined from the calibration model result
P_L	kW	Figure 4.4
N	years	5
r	%	4.5
η_c	%	0.95
η_d	%	0.95
T_0	K	278
$k_{C_{r0}}$	%/cycle	0.001903
$k_{C_{r1}}$	h %/cycle	0.001809
$k_{t,day}$	$\%/\sqrt{\text{day}}$	0.3706
k_t	$\%/\sqrt{\text{min}}$	0.00977
SoC_{min}	%	20
SoC_{max}	%	90

Chapter 5

Results from case study

This chapter contains the results obtained from solving the optimization problem and sensitivity analysis in Julia. The chapter consists of three main sections,

5.1: The main results which include the case study of an EV FCS. This part contains results from simulation for grid reinforcement and a NPV assessment. Besides, it contains an optimization without degradation to estimate the BESS size and simulations with BESS for different BESS capacity and maximum power. The result gives the optimal solution with BESS, and a NPV analysis is done for the optimal case.

5.2: Degradation analysis, which looks into the impact of including degradation. This section contains results from three simulations with optimal BESS size. One where there is no degradation, one with only calender aging and one with only cyclic aging.

5.3: Sensitivity analysis on a random selection of days for spot price, on power tariff, and on the time step. This part contains results from a spot sensitivity analysis, which is used to compute an error estimate for randomly selected spot prices. It also contains results on time step sensitivity analysis, both without degradation and with cyclic degradation, and on grid tariff sensitivity analysis with NPV calculations.

Except for the result of the calibration model, all the analyses are done with the optimization model. For all analyses except time step and spot sensitivity, the time period is five years. The concept of one day representing one month applies for all simulations. Investment analysis is done with NPV assessments. The NPV calculations include operational costs, which are the purchase of electricity on the market and grid tariffs, investment costs, and residual costs.

Simplifications and assumptions are made throughout the chapters so far. The list below contains a summary of assumptions regarding battery degradation and input data.

- The EV charging demand is estimated based on empirical data and stochastic variables, described in section 3.3. It is the load in all the conducted analysis.
- In the calibration and optimization model, the EV charging demand is input and a known variable. Hence a perfect forecast is assumed.
- The spot prices are historical spot prices for the year 2019.
- The BESS is NMC-LMO based and has a charging and discharging efficiency of 95 %.
- The degradation impact as a function of C-rate is approximated as a linear function from the exponential function.
- The temperature is assumed to be regulated at 5 °C, which sets the constants for BESS degradation and causes low calender aging compared to higher temperatures.
- The degradation is only reducing the BESS energy capacity, and the power fade is not included.
- The investment costs for the BESS are calculated based on a projected 2020 price level and an exchange rate of 8.5 NOK/USD.

5.1 Comparison of BESS installation and grid reinforcement

The result of the optimization with load from the case study presented in section 4.1 as input is the content of this section. The case study is the comparison of installing BESS and reinforce the grid for a given load increase at a FCS in Trøndelag.

5.1.1 BESS

The calibration model for a five year period without degradation gives an optimal BESS capacity of 180 kWh and optimal BESS maximum power of 294 kW. The optimal BESS size is the minimum BESS capacity that satisfies the constraints since the dual variables for the relevant constraints are different from zero. For a five year period, assuming 1 FEC on average every day, with C-rate of 1 on average, gives a SoH equal to 80.0 %. By considering this, the minimum BESS capacity needed to be able to provide the necessary energy to keep the grid power below 1250 kW in the fifth year is 180 kWh divided by

0.8. That gives a capacity of 225 kWh. 180 kWh BESS capacity is the minimum energy amount necessary to keep the grid power below the transformer's maximum. Therefore, the estimated initial BESS capacity is 225 kWh to prevent violation of the limit after five years of degradation.

Figure 5.1: Result for optimizing for different BESS power and energy in range 225 to 350 kWh and 300 to 400 kW. The first figure (225 kWh) shows the total costs, while the rest is showing the difference from 225 kWh. The black lines show the accumulated additional costs compared to the figure with BESS capacity 225 kWh. The red line is the cost increase compared to the BESS with minimum cost - 225 kWh and 300 kW.

For the case study, the optimization model, which includes battery degradation, is applied, where the BESS size is a pre-set parameter. The simulations for five years takes typically between 2 and 3 hours for each simulation. The simulation is done for all the combinations of 225, 250, 275, 300, 325, and 350 kWh and 300, 325, 350, 375, and 400 kW. The total costs are for all these combinations shown in figure 5.1. Figure 5.1, as well as 5.7 and 5.9 contains several figures where one is showing the actual costs and used as a reference for the rest. The rest is the difference in cost with respect to the figure with the actual costs. The κ_t values are shown in figure 5.2. Compared to the case with grid reinforcement, these values are about 60 % higher. Figure 5.2 shows that the variations between the different BESS configurations are small. Transformer losses are not a significant fraction of the

total cost, and the cost element is almost invisible in figure 5.1.

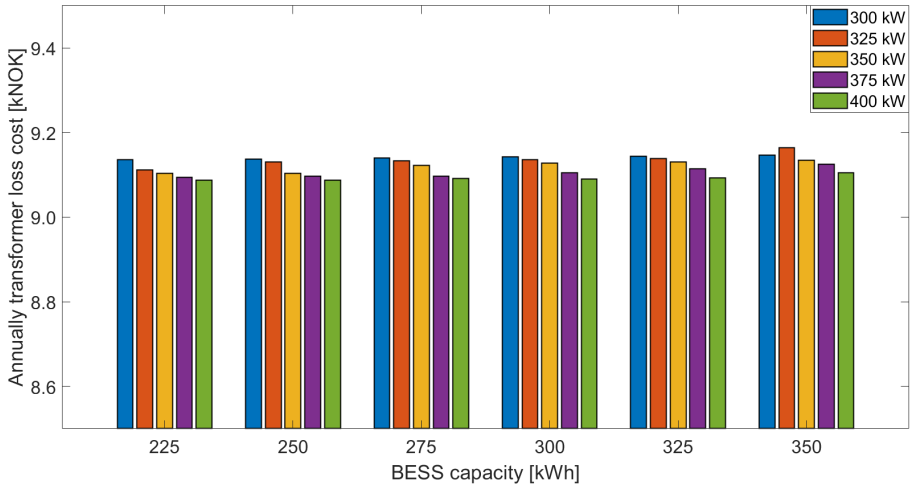

Figure 5.2: Annually transformer loss costs calculated with κ_t for case study with various BESS configurations.

Optimal BESS case

The black graph in figure 5.1 is the gradient of total cost compared to the same battery maximum power for 225 kWh. The red chart is the gradient of total costs compared to the lowest cost, which is the BESS configuration of 300 kW and 225 kWh. The selected BESS configuration for further investigation is the optimal configuration. Figure 5.1 gives that the optimal maximum power and energy capacity of the BESS is 300 kW and 225 kWh. The transformer limit of 1250 kW is in the constraints. This constraint will not be fulfilled for lower energy capacities and thus make the optimization infeasible.

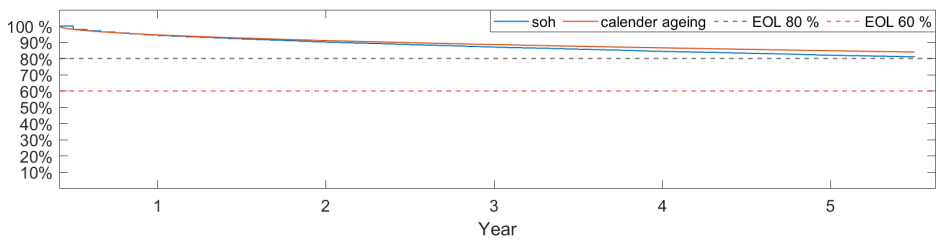

Figure 5.3: SoH for optimal BESS case and calender ageing. EoL criterions as 60 % and 80 % are marked.

The total losses in the transformer are 13 260 kWh during a year, which gives a utilization time κ_t for losses of 1367 hours. For the NPV calculations shown in various tables without the transformer losses. The value of κ_t corresponds to a cost of 41 909 NOK discounted for five years.

Table 5.1 shows the yearly costs and NPV for five years when a BESS is installed. The total costs end up to 11 226 857 NOK. By adding the total transformer loss cost of 41 909 NOK, the NPV for the case of grid reinforcement is 11 267 766 NOK. Figure 5.3 shows the SoH for the case study with optimal BESS size, as well as the calender aging contribution to SoH for the whole time period of 5 years. The assumption that the SoH is 80 % after five years is entirely accurate.

Table 5.1: Yearly costs and NPV calculation for BESS.

	Investment	Operational costs [kNOK]:			Discount	Present	
	costs	Spot	Energy	Power	factor	value	NPV
Year	[kNOK]		tariff	tariff	[%]	[kNOK]	[kNOK]
1	2 040	1262.5	214.7	617.2	100.0	4134.4	4134.4
2	0	1262.2	214.6	617.2	95.67	2003.3	6137.7
3	0	1262.3	214.6	617.2	91.57	1917.6	8055.3
4	0	1262.4	214.6	617.2	87.63	1835.1	9890.4
5	0	1262.5	214.5	617.2	83.86	1756.2	11646.6
6	-510	0	0	0	80.24	-420.2	11226.4

Figure 5.4 shows the power profiles during the first year for four chosen days of the total 12, that represent the month. The BESS power (yellow graph) shows the BESS charging and discharging in order to peak shave in the most cost-efficient way. Figure 5.5 shows the power profile for the same days in the fifth year. The BESS is cutting about the same power as the first year because the maximum power is restricting the ability to cut more the first year. It is theoretically possible to provide more energy in the first year because the BESS capacity is higher than the last year. The optimization model gives the optimal solution, and thus the reason is that it doesn't provide any economic advantages.

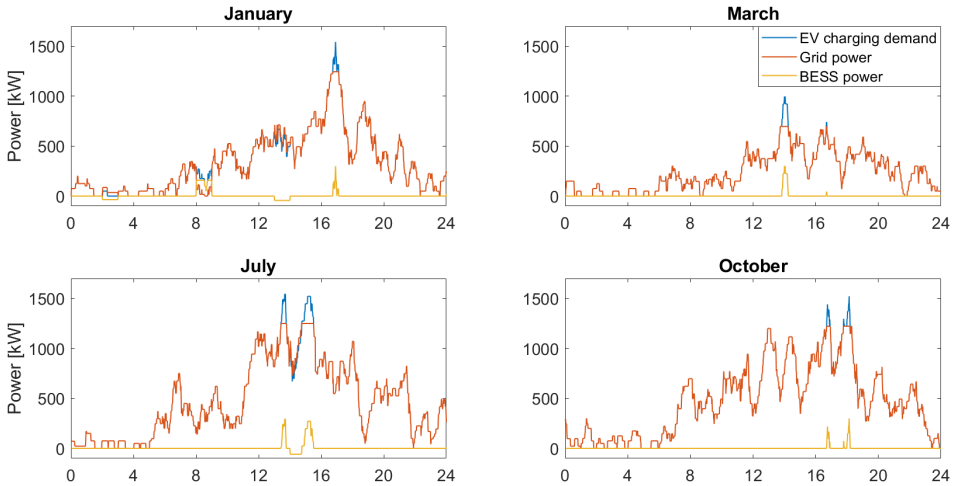

Figure 5.4: Power profiles for 4 chosen days the first year - January, March, July and October. The shown day is the one that represents the month.

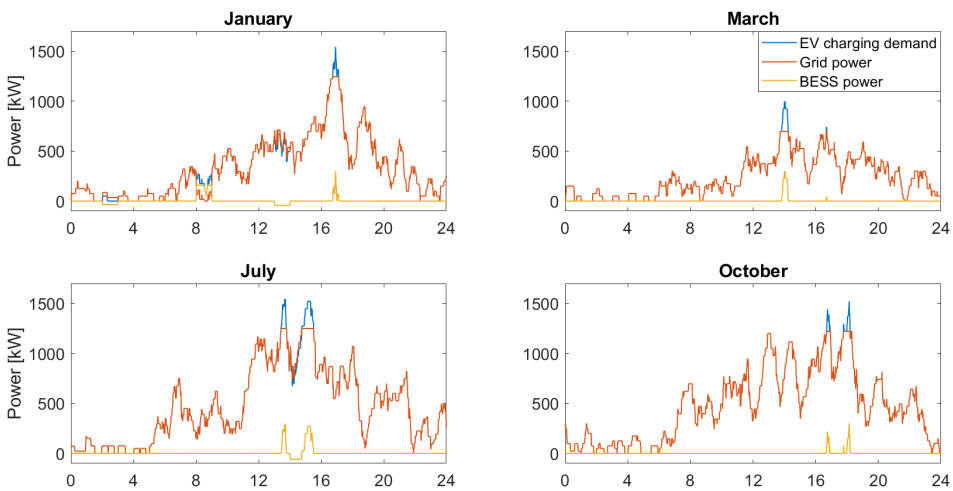

Figure 5.5: Power profiles for 4 chosen days the fifth year - January, March, July and October. The shown day is the one that represents the month.

5.1.2 Grid reinforcement

The EV FCS today has a peak power of 1044 kW. The case study looks at a 50 % increase of chargers, which will increase the peak power to 1544 kW. If the FCS operator does not invest in a BESS, the operator will be forced by the DSO to finance a new transformer at the substation because the existing substation's rating is 1250 kW. The new transformer at

the substation needs to have a capacity of 1600 kVA.

The peak power at the FCS is 1544 kW, and the losses in the transformer are 11 065 kWh a year. The ΔP_{max} is 13.1 kWh per hour [44] and corresponds to an annual κ_t of 845 hours. The value of κ_t gives a total cost of transformer losses of 45 039 NOK discounted for five years. The investment costs are the costs of buying a new transformer, subtracted by the residual value. The residual value of the existing transformer is 250 000 NOK, and a new 1600 kVA transformer is assumed to cost 500 000 NOK. The difference between the cost of a new transformer and the residual value of the old one is set to be the investment cost, which is 250 000 NOK. By assuming the lifetime of the transformer of 30 years and a linear decrease in value, the residual value of the new transformer after five years is 416 000 NOK. Table 5.2 shows the yearly costs and NPV for a 5 year period.

Table 5.2: Yearly costs and NPV calculation for grid reinforcement.

	Investment	Operational costs [kNOK]:			Discount	Present	
	costs	Spot	Energy	Power	factor	value	NPV
Year	[kNOK]		tariff	tariff	[%]	[kNOK]	[kNOK]
1	250	1264.3	214.3	788.6	100.0	2767.2	2517.2
2	0	1264.3	214.3	788.6	95.67	2169.0	4686.2
3	0	1264.3	214.3	788.6	91.57	2076.1	6762.3
4	0	1264.3	214.3	788.6	87.63	1986.7	8749.0
5	0	1264.3	214.3	788.6	83.86	1901.3	10650.3
6	-416				80.24	-333.8	10316.5

The discounted operational and investment costs without BESS are 10 316 850 NOK. By adding the total transformer loss cost of 45 039 NOK, the NPV for the case of grid reinforcement is 10 361 889.

5.1.3 Comparison of BESS and grid reinforcement

The NPV for grid reinforcement is 10 361 889 NOK and for BESS installation 11 267 766 NOK. That corresponds to a difference of 905 877 NOK. The transformer loss costs for grid reinforcement is 45 039 NOK and for BESS installation 41 909 NOK, which corresponds to a difference of 3 130 NOK. However, the energy losses are slightly higher

for the BESS case than for the grid reinforcement, with a difference of 2 195 kWh annually. The κ_t is 60 % bigger when using BESS than reinforcing the grid. The losses at rating power for a 1250 kVA transformer are less, around 70 % of a 1600 kVA, than for a 1600 kVA transformer.

Figure 5.6 shows the difference between the case of BESS and grid reinforcement and contains the same numbers as discussed above. The monthly cost difference is the costs of BESS subtracted by the cost of grid reinforcement. The costs include operational and investment (and residual) costs and not transformer loss costs.

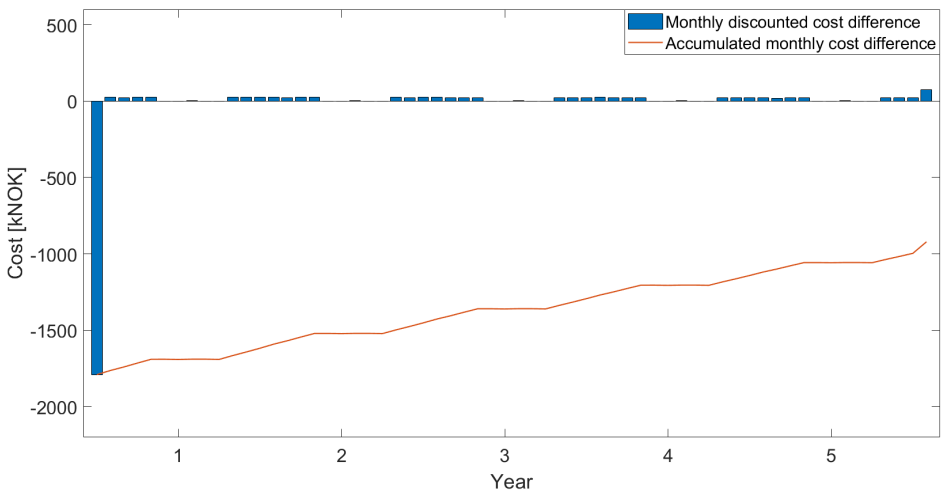

Figure 5.6: NPV difference between grid reinforcement and BESS installation. The cost difference is the cost of grid reinforcement subtracted the cost of BESS installation. A negative accumulated cost at the end means that the resulting NPV of the costs of installing a BESS is higher than grid reinforcement.

5.2 Degradation analysis

Some test runs are done with the optimization model in section 3.2.3 for a period of five years to perform an analysis of the impact of degradation. The battery size and power are pre-determined and are the optimal case of 225 kWh and 300 kW. The three test runs are:

1. one is without any degradation (D0)
2. one is with only calender aging (D1) and
3. one is with only cyclic aging (D2).

A comparison of these cases estimates the impact of degradation. The optimization model

has only operational costs in the objective function, thus no investment costs as the overall model in section 3.2.3.

For the first case without any degradation (D0), the $SoH(t)$ is set to 1 for all $t \in T$ in constraint 3.13e. Thus the BESS has a constant energy storage capacity equal to E_{B0}, which can be seen from constraint 3.13e. Constraint 3.13h, 3.13i and 3.13j are omitted. Since all degradation-related constraints are removed, the optimization problem becomes completely linear.

For the next couple of runs (D1 and D2), the cyclic and calender degradation distinctly investigated. The optimization model is applied to simulate the different degradation mechanisms. With only calender aging (D1), the only difference from the case study is that $f_c(t)$ is set to 0 for all $t \in T$ and eliminate all cyclic aging. For D2, the only difference from the case study is that k_t is set to 0, and thus remove all calender aging.

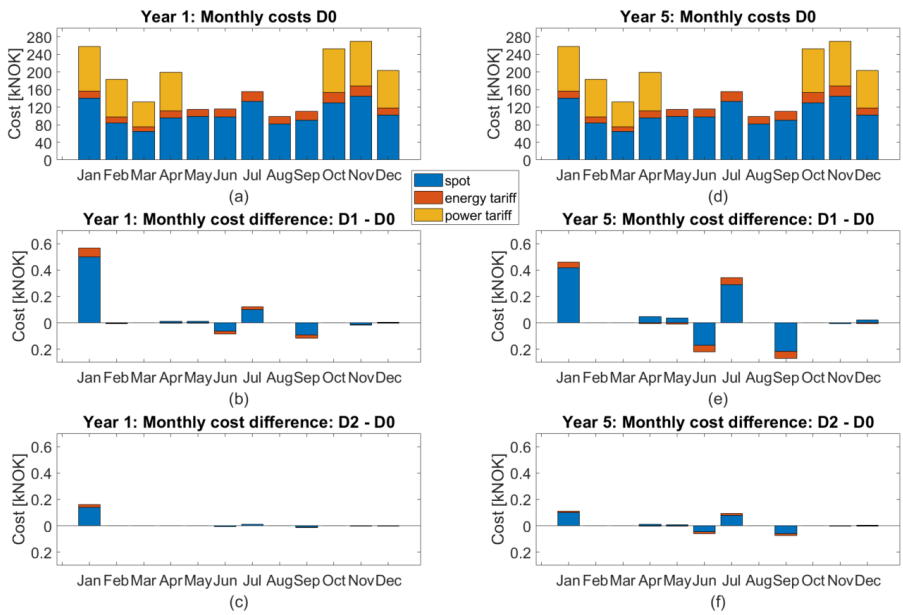

Figure 5.7: Economic result of the optimization model for degradation analysis. D0 - no degradation, D1 - calender degradation and D2 - cyclic degradation. (b) and (c) is the economic result the first year subtraced for the case with no degradation, shown in (a). (e) and (f) is the same for the fifth year

5.2.1 No degradation

Figure 5.7 (a) shows the operational costs. The total cost for the first year is 2 093 795 NOK. The BESS discharged 45.08 MWh and charged 49.28 MWh through the year and

thus had a charging and discharging loss of 4.21 MWh. In the fifth year, the operational cost is 2 093 783 NOK.

5.2.2 Calender ageing

Figure 5.7 shows the operational costs. The final SoH value of the year is 92.91 %. The total cost for one year is 2 094 273 NOK. The BESS discharged 44.07 MWh and charged 48.75 MWh through the year and thus had a charging and discharging loss of 4.68 MWh. In the fifth year, the total operational cost is 2 094 177 NOK.

Compared to the total operational costs for D0, including calender aging raises the costs by 478 NOK the first year and 394 NOK the last year, which corresponds to an 0.022 % increase and 0.019 % increase respectively for the first and last year.

5.2.3 Cyclic ageing

Figure 5.7 shows the operational costs. The final SoH value of the year is 99.11 %. The total cost for one year is 2 093 939 NOK. The BESS discharged 45.00 MWh and charged 49.43 MWh through the year and thus had a charging and discharging loss of 4.43 MWh. The last year the total operational cost is 2 093 870 NOK.

Compared to the total operational costs for D0, including calender aging raises the costs by 144 NOK the first year and 87 the last year, which corresponds to an 0.007 % increase and 0.004 % increase respectively for the first and last year.

Summary of degradation analysis

The degradation analysis shows the impact of degradation in the first and last year. The calender aging is determined in this case because the temperature is assumed to be constant. The cyclic aging depends on operational behavior. The calender aging is much higher than the cyclic aging the first year. After a few years, the calender contribution to aging is less, as seen in figure 5.3 from the case study. It shows five years of degradation where the domination of calender aging can be seen in early periods.

5.3 Sensitivity analysis

This section includes the results of varying some variables which are set in the main case and investigates how it impacts the overall costs. It provides sensitivity analysis on the spot price, time step, and grid tariff. Table 4.4 show the system and simulation parameters

for the case study where BESS installation and grid reinforcement are compared. Table 5.3 gives an overview of the sensitivity analysis.

Table 5.3: Change in parameters compared to case study to conduct sensitivity analysis. E_{B0} and P_{inv}^{max} are the set to optimal values determined from the case study.

Analyze	Parameter	New value
Spot	c_{spot}	Figure 5.8
Time step	P_L	Figure 4.7
Grid tariff	$c_{P,tar}$, $c_{E,tar}$	Table 5.7

The spot sensitivity analysis is different from the other sensitivity analysis. The spot sensitivity is to quantify the weakness of picking a random day to represent the month, which is classified as a weakness of the model. Since one day represents one month, it is necessary to pick a day of spot price representing that month as well. The ideal model would have included every day. However, as mentioned in previous chapters, this is not possible for long-term optimization due to computational limits.

5.3.1 Sensitivity on spot price

This section will quantify the possible errors due to the random selection of a day of spot price representing one month. The BESS configuration is the optimal one, 225 kWh and 300 kW. The four cases are denominated as a,b,c,d. The dates which are randomly picked from the historical 2019 spot prices for the spot sensitivity analysis are shown in table 5.4.

Table 5.4: Dates chosen in the sensitivity analysis, randomly picked weekdays from 2019 spot prices. All the prices are shown in figure 5.8.

Case	Jan	Feb	Mar	Apr	May	Jun	Jul	Aug	Sep	Oct	Nov	Dec
a)	13	1	27	5	3	9	15	5	28	10	9	3
b)	10	8	22	1	2	20	18	16	21	23	23	10
c)	7	10	4	16	10	6	5	28	20	13	28	4
d)	27	5	29	16	23	28	9	14	13	24	24	4

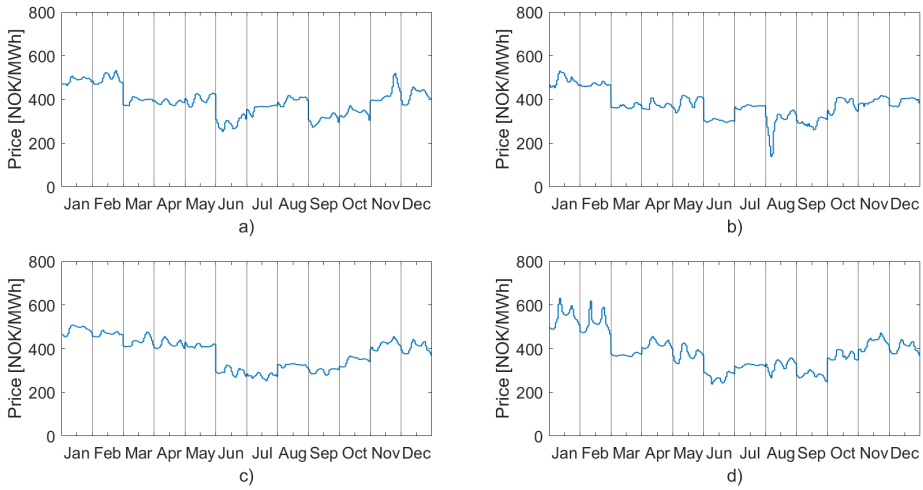

Figure 5.8: Randomly selected prices for spot sensitivity analysis. There are four cases, a)-d), which will be used in four independent optimizations.

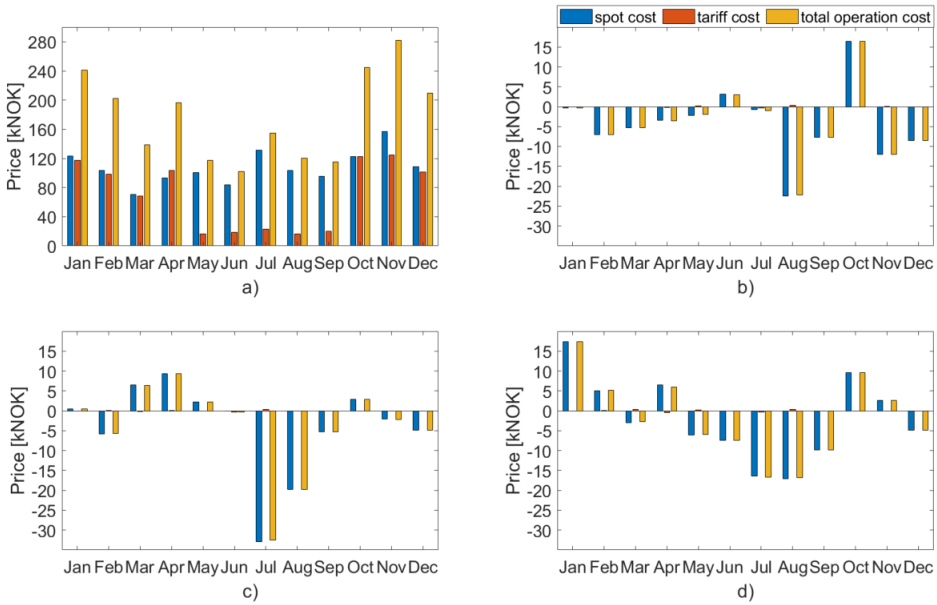

Figure 5.9: Sensitivity analysis: economic result for the four cases a)-d). a) contains the acutal cost, while b) to d) is the difference in those cases wirh respect to a).

Figure 5.8 shows four instances where there has been randomly chosen a day to represent each month. When the spot price is randomly chosen, an error estimate is made by con-

ducting a sensitivity analysis based on section 2.4. Figure 5.8 shows four cases a)-d) where a day with spot prices are chosen randomly to represent each month, which is used in the sensitivity analysis. By running one year for all the cases a)-d), the financial result of these 4 cases is presented in figure 5.9. Based on that result, an empirical standard deviation σ is calculated with equation 2.24 presented in subsection 2.4.

Numerical values of the total costs are shown in table 5.5 which also includes the final SoH values. Figures in table 5.5 gives an average operational cost $\bar{C}$ of 2 094 463 NOK by applying equation 2.25. By applying equation 2.24 with the figures in table 5.5 and the average cost $\bar{C}$, the standard deviation σ is calculated to be 23 901 NOK. The relative error ε is then 1.14 % given from equation 2.26.

Table 5.5: Sensitivity analysis results.

	Unit	Case a)	Case b)	Case c)	Case d)
Total operational cost	[NOK]	2 125 195	2 075 236	2 075 798	2 101 622
Deviation from $\bar{C}$	[%]	1.46	0.92	0.89	0.34
SoH after one year	[%]	92.13	92.24	92.26	92.05

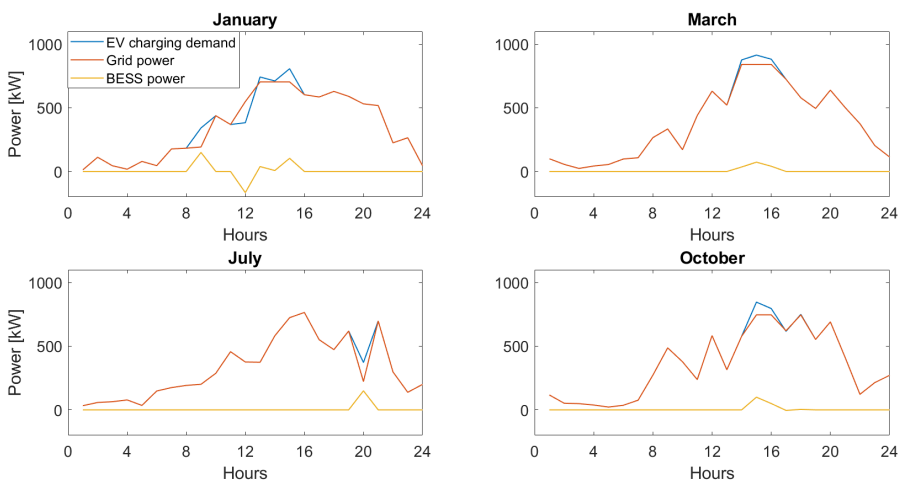

Figure 5.10: With no degradation, the EV charging demand, grid power and BESS power is shown for 4 chosen days - January, March, July and October. The shown day represent the month.

5.3.2 Sensitivity on time step

The choice of the time step is an object for a sensitivity analysis to investigate the consequence of that choice. The decision in this thesis was to use minute resolution. The sensitivity analysis shows the impact on the total costs if the time step interval instead is in hours. One case of no degradation and one with cyclic degradation are considered. All constants affected by the time step are corrugated. The optimization period is one year.

Table 5.6: Results from optimization without degradation mechanisms with both minutes and hours as resolution.

Variable	Unit	Value min resolution	Value hour resolution	Difference
BESS discharged	[MWh]	45.08	54.89	-9.81
BESS charged	[MWh]	49.28	59.82	-10.54
BESS loss	[MWh]	4.21	4.93	-0.72
Grid energy	[MWh]	3 296.29	3 121.19	175.1
		Costs		
Spot	[NOK]	1 261 985	1 203 070	58 915
Energy tariff	[NOK]	214 589	203 190	11 399
Power tariff	[NOK]	617 221	422 530	194 691
Total cost	[NOK]	2 093 795	1 828 790	265 005

The time step analysis is done with the optimization model with the same modifications as for D0, now at h instead of t and H instead of T. The EV charging demand is therefore changed with the resulting charging demand shown in section 4.2.3. Running the optimization model with an hourly time step, figure 5.10 shows the resulting power profiles.

Table 5.6 shows the two test runs with no degradation, one with a minute resolution, which is presented in subsection 5.2.1, and one with an hourly resolution, shown in this section. From table 5.6, it can be seen that the difference in costs for one year is 265 005 NOK. This corresponds to an additional cost of 14.5 % when the simulations are done with minute resolution compared to hourly resolution. The power tariff costs are 194 kNOK less with an hourly time step. However, the level of peak shave with the hourly resolution is lower

than minute resolution, as shown in figure 5.11.

Regarding calender aging, it will give the same result since it does not depend on any other variable than time. In the case of cyclic aging, the other time resolution may impact the SoH differently. To investigate this, the model with hour resolution is run for a year with cyclic degradation constraints, which is given in equation 3.13h, 3.13i and 3.13j, with time step h instead of t. The result can then be compared to the results of D2 to see the difference in FEC and the final SoH for the two different time steps.

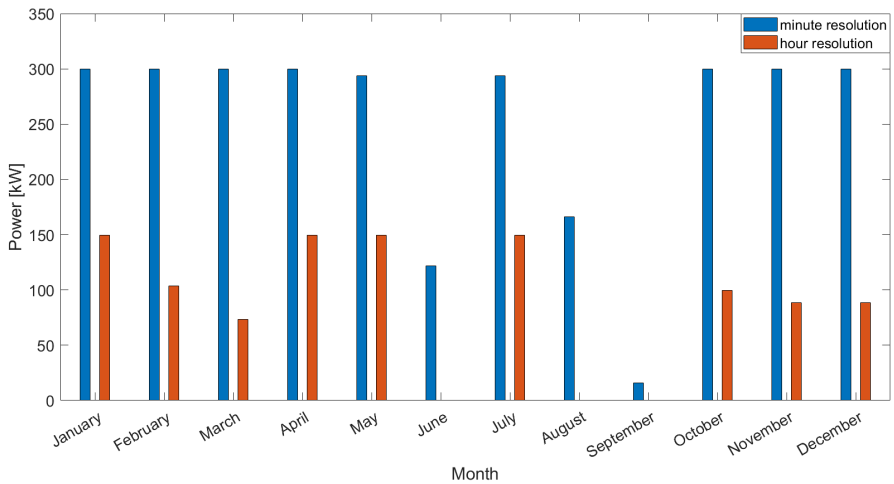

Figure 5.11: Peak shave with hourly and minute resolution.

Running the optimization model with time step intervals in hours, now with cyclic degradation, results in 271.4 FEC during one year and a decrease in SoH of 0.62 %. Compared to the result of D2, which has a SoH reduction of 0.9 % and 394.1 FEC, there is a noteworthy difference. By looking at the relationship between the SoH reduction and FEC, the impact of the C-rate function can be investigated. For hourly time resolution this number is 2.26 $\cdot 10^{-3}$ and for minute time resolution 2.28 $\cdot 10^{-3}$. The average C-rate for the two different time resolutions is about the same. The only explanation to the different final SoH is not different C-rates, but different numbers of FEC.

5.3.3 Sensitivity on grid tariff

The last sensitivity analysis is done concerning the tariffs, both energy and power tariff. In the case study of a FCS, the grid tariffs are based on the DSO in the region, Tensio's, tariffs. To make a sensitivity analysis of this, the tariffs from Norway's largest DSO, Hafslund, is used [52]. The optimization model is used as presented in section 3.2.3 for the same

battery sizes to run with these tariffs. Hafslund has a different set up of the energy and power tariffs, as shown in table 5.7.

Table 5.7: Alternative grid tariff regime.

	Fixed fee [NOK/month]	Energy tariff [NOK/MWh/month]	Power tariff [NOK/kW/month]
December - February	1065	70	150
March & November	1065	70	80
April - October	1065	39	23

The optimal BESS configuration is the same when the alternative grid tariff regime is applied. The BESS capacity is 225 kWh and maximum BESS power 300 kW, corresponding to the minimum BESS size to keep the maximum grid power at 1250 kW. The economic costs for both BESS installation and grid reinforcement with the alternative grid tariff regime are higher compared to the total costs in the case study. However, by running the case of no BESS (grid reinforcement) for this grid tariff regime, it can be compared to the BESS case of the alternative grid regime.

Table 5.8: Yearly costs and NPV calculation for grid reinforcement with alternative grid tariff regime.

	Investment	Operational costs [kNOK]:			Discount	Present	
	costs	Spot	Energy	Power	factor	value	NPV
Year	[kNOK]		tariff	tariff	[%]	[kNOK]	[kNOK]
1	250	1264.3	167.0	1068.5	100.0	2749.8	2749.8
2	0	1264.3	167.0	1068.5	95.67	2391.6	5141.4
3	0	1264.3	167.0	1068.5	91.57	2289.1	7430.5
4	0	1264.3	167.0	1068.5	87.63	2190.6	9621.1
5	0	1264.3	167.0	1068.5	83.86	2096.3	11717.4
6	-416				80.24	-333.8	11383.6

Table 5.9: Yearly costs and NPV calculation for BESS with alternative grid tariff regime.

Year	Investment costs [kNOK]	Operational costs [kNOK]: Spot	Energy tariff	Power tariff	Discount factor [%]	Present value [kNOK]	NPV [kNOK]
1	2 040	1262.8	167.2	837.8	100.0	4307.8	4307.8
2	0	1262.4	167.1	838.0	95.67	2169.3	6477.1
3	0	1262.5	167.1	838.1	91.57	2076.5	8553.6
4	0	1262.6	167.1	838.2	87.63	1987.4	10541.0
5	0	1262.7	167.1	838.4	83.86	1902.1	12443.1
6	-510	0	0	0	80.24	-420.2	12022.9

Table 5.8 and 5.9 shows the yearly costs and discounted costs for five years for those two cases. Figure 5.12 shows the discounted cost difference between the two options with alternative grid tariffs. The accumulated cost difference, which is equivalent to the NPV difference, is 639 kNOK in the advantage of reinforcing the grid.

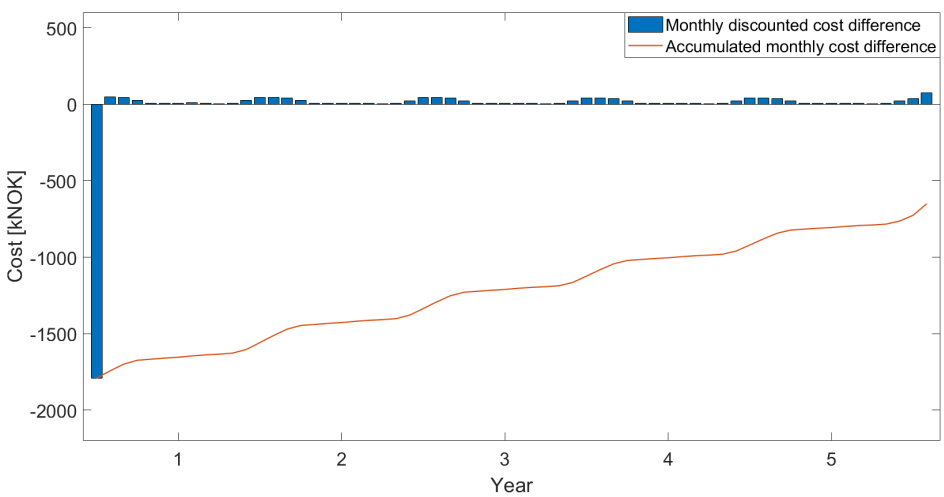

Figure 5.12: NPV difference between grid reinforcement and BESS installation with alternative grid tariffs. A positive bar or value means that the cost is higher for grid reinforcement.

The transformer losses in this case of changed grid tariffs are in the same size of the order as for the case study. κ_t is 845 hours for grid reinforcement and 1357 for using BESS. The discounted costs for transformer loss is 45 040 NOK for grid reinforcement and 41 796 NOK for BESS.

The remaining capacity during the five years is shown in table 5.10, and the final SoH value is 80.45 %. The alternative grid tariffs lead to higher utilization of the BESS, which is evident from comparing to the remaining capacity for the case study. Table 5.10 shows the numeric values.

Table 5.10: BESS capacity at the beginning of each year with alternative tariffs.

	BESS capacity [kWh] in	
Year	Case study	Alternative grid tariffs
1	225.0	225.0
2	209.2	207.3
3	199.6	199.0
4	193.2	192.3
5	187.6	186.4
6	182.5	181.0

For a BESS capacity of 225 kWh, which is the optimal case, the change in cost per kW is 2018 NOK/kW for the alternative grid tariffs and 2060 NOK/kW for the main case. For the highest BESS capacity, 350 kWh, the same change in cost is 1099 NOK/kW for the alternative tariffs and 1451 NOK/kW for the main case.

Chapter 6

Discussion

The chapter discusses the result of the case study to compare installing a BESS or reinforce the grid. It also discusses the sensitivities and impact of degradation on the financial outcome. The main findings from chapter 5 are discussed as well as the model and the assumptions which are made.

6.1 BESS versus grid reinforcement

Given the outcome of the NPV calculations for reinforcing the grid and installing BESS, the difference is 906 kNOK in favor of reinforcing the grid. The difference in investment costs is high. The net investment cost is 1700 kNOK higher for the BESS. Installing BESS provides around 800 kNOK of operational cost savings since the end NPV difference is 900 kNOK. The power tariff costs are substantially reduced by applying a BESS due to reduced peak power. The peak power is reduced by 19 % for the months with the highest power peaks. With another grid tariff regime, the cost savings will be different, and the result from the grid tariff sensitivity analysis is discussed in section 6.3.

Energy arbitrage and energy-related cost elements

The costs of buying electricity referred to as spot costs are slightly lower when BESS is installed. The advantage of that is energy arbitrage. The BESS stores energy buying in cheap time periods and discharging when necessary to peak shave; however, these are time periods where the spot price is typically higher. The energy tariff is, on the other hand, higher when installing BESS. The energy tariff is not varying daily and is paid

independently of when the energy is bought. Due to charging and discharging losses when applying BESS, more energy is drawn from the grid when installing a BESS. Thus, the energy tariff cost is slightly higher than for the case of grid reinforcement. Summing up these two discounted cost elements, the BESS has 7 kNOK lower costs connected to energy-related costs compared to grid reinforcement. The cost savings equals 0.06 % of the total cost for BESS. In this case, the advantages of buying at cheaper hours are higher than the disadvantage of additional energy tariffs for losses due to charging and discharging losses of the BESS. In sum, the FCS operator saves costs from power tariff and purchasing energy from the market but pays a higher energy tariff. If the spot price varies more than the spot price used in this case study, the effect of energy arbitrage will be higher. In this case, it can be seen in figure 4.10 that mainly two months have high fluctuations in the spot price, which is January and June. From May to September, the power tariff is zero. In figure 5.6, a small bar in July is visible, which means that there is some cost saving from installing a BESS this month. July is seen in figure 5.4, where it can be seen that the net BESS energy is discharged. Since one day represents one month, the spot price for when the BESS charged in June. The spot price in figure 4.10 shows that June has a low price. Thus, the cost savings in July are from charging and storing energy from June, to discharge in July. It gives cost savings since a lot less energy is bought in July compared to the load and the case of grid reinforcement.

The optimal solution is on two constraints, the lower limit for BESS power and energy capacity. An optimization model that does not include the alternative cost or the lower grid limit of 1250 kW has another solution with a smaller BESS as an optimal solution. Figure 5.1 shows that. The red line, which is the overall cost function, clearly shows a pattern that a smaller BESS configuration is optimal. The requirement of keeping the grid power below 1250 kW makes a solution with a smaller BESS infeasible.

Spot sensitivity analysis

Energy arbitrage is fundamentally the same as the spot sensitivity. The question is, how much does the spot price impact the total economic cost. The sensitivity analysis on spot price ends up with a relative error of 1.14 %. There are two ways to interpret the deviation from the average total cost. Either as an error estimate of picking a random day to represent the spot prices for a month or as potential uncertainty of using BESS for energy arbitrage. However, by interpreting the result with the last interpretation, the premise for selling energy is not high prices, but peak shaving. The relative error from randomly select spot price is about 20 times higher than the impact of net savings from the sum of the energy losses in the battery and energy arbitrage. Changes in spot price impact more on the overall cost for BESS and grid reinforcement rather than the difference between them,

which comes from energy arbitrage. Figure 5.9 shows the impact of different spot prices, and it shows a random and changing pattern. The energy tariff costs are barely seeable at some months since the difference in charged energy is not present; it is only a change in the cost of buying electricity at spot price.

By comparing the spot prices in figure 5.8 and the economic result in figure 5.9, som considerations are done for the spot sensitivity analysis. Case d) had a more expensive January than all the three others but a cheap summer, and compared to the spot prices, it is reasonable. January and February had high price fluctuations in case d). The high price fluctuations would give some extra income for both BESS and grid reinforcement for that spot price. The results for case b) and c) show that in these cases, there is summer with lower spot prices than case a), as can be seen from the spot prices. Table 5.5 shows the results for each case, and case a) is the one with the highest deviation from the average cost with 1.46 %. Case b) and c), which have the lowest costs deviate 0.92 % and 0.89 % from the average costs while case d) is only deviating 0.34 % and has a cost quite close to the average cost. Since the costs are all from the same year, only different days in the month, the deviation is measured over a time period within a year. A comparison for spot prices from many different years will give a more satisfying picture of the potential in energy arbitrage. However, it is clear from the spot sensitivity analysis that the potential for the big cost savings from energy arbitrage is not present. The error estimate is not accurate by looking at four cases and only gives a sign of the range the impact the random selection on spot prices have.

Energy losses

The expected transformer losses are to be higher when the existing transformer is in use, and a BESS is applied. Installing a BESS will make the grid power more often to be at the transformer's rating power. The expected scenario is what happens in the case study, and figure 5.2 shows the utilization cost of transformer losses when installing a BESS. With higher maximum BESS power, the transformer losses decrease. With higher BESS capacity, the transformer losses increase slightly. The reason for the last comment is that the grid power is on average at high levels for a larger BESS. The BESS charges and discharges more energy and is in that period at high power levels for a long time since the losses are quadratic. However, the differences in transformer losses for different BESS configurations are low, the difference between BESS configurations that results in the highest and lowest is around 0.1 kNOK annually.

The installation of BESS gives 60 % higher utilization losses compared to reinforcing the grid. The loss rating is less for the small transformer, so the losses when the transformer operates at rated power are less compared to a transformer with a higher power rating.

The actual losses are 2195 kWh more in the case of BESS. However, due to higher loss ratings for bigger transformers, the costs for power losses are higher for grid reinforcement than for BESS installation. However, the actual losses for BESS installation are lower compared to grid reinforcement. The cost of transformer losses is respectively 45 kNOK and 42 kNOK for grid reinforcement and BESS installation. The transformer losses are not a substantial part of the total economic cost and counts for respectively 0.43 % and 0.37 % of the total costs. Economically, installing a BESS will lead to that energy losses are a smaller part of the costs in contrast to the actual losses in kWh, which are higher.

Impact from reduced battery prices in the future

Since the investment costs are high, a small consideration is done around further decreasing battery costs. If the price on BESS is reduced as the projections show in 2.3, the price in 2025 is about 450 USD/kW and 130 USD/kWh. With an exchange rate of 8.5 NOK/USD, the price is 3825 NOK/kW and 1105 NOK/kWh. For the optimal BESS size (225 kWh and 300 kW), the investment costs will be 643 875 NOK lower. The price reduction will have a direct and highly impactful effect on the NPV difference. The residual value will be 160 969 NOK lower. Thus the net decrease is 483 kNOK. The NPV difference of 900 kNOK in the case study will be reduced to 417 kNOK, however still in the advantage of grid reinforcement. In a few years, the calculations will be quite different if the projections are realized.

Comparison to other work

There are some differences in the results and assumptions of this case study compared to the other studies presented in the chapter 1 ([9], [10] and [11]). Reference [9] and [10] look into when the BESS does grid services and peak shaving and concludes that the BESS has a net positive effect. However, a 30 % decrease in battery investment cost is needed to have a profitable case, which is a lower decrease than needed in the result from the case study in this thesis. The assumed costs for the AC/DC converter is 200 €/kW and far less than assumed in this thesis. Operational cost savings are the main contributing factor in all cases, and the profitability is set up to the investment cost. Therefore the assumed investment cost impacts the conclusion on profitability by installing a BESS. Installing a BESS and its profitability must be investigated in each specific case based on the battery prices available and the estimated cost savings. Reference [11] concludes that for the specific case of a Norwegian swimming pool facility, installing a BESS is profitable. Degradation was taken into account by incorporating a degradation cost element in the objective function.

By including the degradation, an over-dimensioned BESS is necessary for it to be able to

peak shave the inevitable power peaks. Thus, degradation results in a higher investment cost than assumed without considering capacity fade. As introduced in subsection 2.1.2, it is possible to put degradation as a cost element in the objective function. However, the additional investment cost needed is not considered when making the cost estimate for degradation. The additional investment cost should, therefore, be included in that cost element if the degradation is a pure cost element in the objective function.

6.2 Eonomic impact by including degradation and increased time step

The degradation analysis consists of three models, D0 (no degradation), D1 (only calender aging), and D2 (only cyclic aging). The results are presented in section 5.2.

Degradation analysis

The results in section 5.2 gives a picture of a small economic impact. The highest financial difference is from calender aging. However, it is relatively small compared to the operational costs. The increase in operational costs when including calender aging is about 0.02 % higher. There is a reason why this is not impacting that much in this case. The minimum BESS size (and the optimal) is set to 225 kWh because of the first simulation without degradation, and with BESS size as a variable, gave the result of 180 kWh BESS capacity as optimal. The resulting BESS capacity was divided by an estimated SoH of 80 % to ensure that the energy capacity was sufficient after five years of operation. The BESS must be able to provide enough energy to peak shave the necessary power to keep the grid power below 1250 kW. This estimation method succeeded in ensuring that the BESS had enough energy to peak shave. The maximum power of the BESS was 300 kW, and maximally utilized to reduced power tariff costs. Figure 5.1 shows that the savings of power tariffs with increasing BESS maximum power did not cover the increasing investment costs of the BESS. However, when the investment was made, it is utilized to minimize the cost, thus minimize the grid power tariff.

Cyclic aging

In the case study, the degradation mechanisms did not make a direct seeable impact on the financial result. Both calender and cyclic aging had tiny deviations from the case of no degradation. The simulation verified that calender aging is the main aging effect and dominates cyclic aging in the short-term.

The cyclic aging has a long term impact on battery degradation, and it is necessary to have

a detailed model of degradation. The economic impact is, as mentioned, small in this case. Mainly because the dimensioning of the BESS is to ensure that the BESS can provide enough energy to peak shave a wanted level for the five year period. It is also affected by the fact that the power capacity of the BESS is constant, which limits the potential of peak shaving. For a case when the energy capacity is not over-dimensioned for the first years to peak shave, this will have another impact on the result. C-rate is included to incorporate degradation details, to scale the degradation. A discussion on C-rate and FEC for the first year of D2 and the time step sensitivity model with cyclic degradation will follow to slide over to time step analysis.

Hourly versus minute time resolution with cyclic degradation

This paragraph discusses the result of D2 in section 5.2, which has time step in minutes, compared to the result in section 5.3.2, which shows the result of D2 with time step in hours.

By using a time step in hours, the financial result for the first year is 14.5 % higher when the time step is in minutes. The average C-rate is not changing much between the two different time resolutions, but the number of FEC is. The number of FEC is about 45 % higher in the case of minute resolution compared to hourly resolution. It corresponds one to one with the difference in SoH between the two cases. The SoH reduction is 45 % higher in the case of minutes resolution compared to hourly resolution. The answer to this significant difference is found in the power profiles for the first year in figure 5.4 and figure 5.10. By looking at the BESS power, there are many small fluctuations on the minute scale and none with hourly resolution. These fluctuations are the reason why the number of FEC is different. Information on power peaks and small variations in the load is lost, which massively impacts the economic outcome and degradation analysis, using hourly resolution.

Hourly versus minute time resolution with no degradation

This paragraph discusses the result of D0 in section 5.2, which has time step in minutes, compared to the result in section 5.3.2, which shows the result of D0 with time step in hours.

By looking at the yearly difference in using time step in hours instead of minutes with no degradation is also having an impact on the financial result. Subsection 5.3.2 shows an increased total operational cost of 14.5 % if the time step intervals are in minutes instead of hours. Again, power tariffs are a substantial contributor to reduced costs. Around 75 % of the total cost difference is due to the power tariff. The selection of days to represent the

month is made after the transformation from minutes to hours. Therefore, most of the days are different in the case of hourly resolution than minutes resolution. Figure 4.9 in chapter 4 shows that the power peaks of the EV charging demand are substantially reduced, and thus even without a BESS, the power tariff costs would be reduced. Figure 5.11 shows the peak shave for both time resolutions. It is evident that the BESS peak shave abilities are lower when the EV charging demand is given in hours. Thus the cost savings compared to grid reinforcement will be lower.

6.3 Grid tariff's impact on BESS profitability

This section discussed the results obtained from a grid tariff sensitivity analysis, where the results are presented in subsection 5.3.3. The results are a comparison of installing BESS and reinforce the grid with a different grid tariff regime. The alternative grid tariffs are more expensive for the FCS operator and give higher income to the DSO. The power tariff is never zero and varies over the year, where the winter months are costly, about 2.3 times more expensive than in the case study.

Economic outcome with alternative grid tariff

The alternative grid tariffs make the electricity bill higher for the FCS operator and income for the DSO higher, in both cases, installing a BESS and reinforcing the grid. By installing a BESS with an alternative grid tariff regime, the total cost is 12 022 kNOK, which is 6.7 % more expensive than installing a BESS in the case study. For alternative grid tariffs, installing BESS compared to reinforce the grid, the NPV difference is 639 kNOK in favor of the grid reinforcement. Thus the NPV difference between the two options to meet increased load demand reduces with 29.5 % compared to the NPV difference in the case study. The future price scenario for 2025 with a net investment decrease of 483 kNOK implies a NPV difference of 156 kNOK in the case of alternative grid tariffs.

Dual variables for BESS

Another indication of the increased profitability of the alternative grid tariffs is the change in cost per kW for higher BESS capacities. These numbers are equivalent to dual variables if the BESS size was a variable. For a 225 kWh BESS, the difference of the expenses per kW is significant because of the constraint of maximum grid power of 1250 kW and thus a minimum BESS power capacity of 300 kW. For a 350 kWh BESS, the change in cost per kW is lower compared to a 225 kWh BESS, and with alternative grid tariffs, the difference in cost is 24 % lower compared to the grid tariff in the case study. Thus, higher and more expensive grid tariffs increase the profitability of using BESS. The last observation

which should be highlighted in terms of power cost savings versus energy capacity is the EV charging demand. In this case, the EV charging demand is highly fluctuating, and thus a cut of 1 kW during peak hours requires low energy amounts. The optimal BESS configuration depends a lot on the profile and characteristics of the power demand.

Future grid tariffs

The grid tariffs in Norway are under development. The applied and discussed grid tariffs in this thesis is for a commercial customer. NVE, the regulator, published on February 2nd, 2020, a new suggestion for the grid tariffs for households [53]. It contains new main ideas that are likely to be approved, and the most fundamental shift is to have a tariff more based on power than earlier. This tariff regime creates incentives for the customer to minimize the peak power and, for example, invests in BESS.

6.4 Value for DSO

This section of discussion is provided to discuss the value and challenges BESS installations could mean for the DSO. The value for DSO is to see the BESS installation from a socio-economic view and a grid perspective.

First of all, when a customer installs a BESS to peak shave, the DSO loses revenue. The DSO's income is used to upgrade the grid. On the other hand, a peak shaving BESS contributes to a lower need for doing grid upgradations. The charging and discharging losses of the BESS, in addition to increased transformer losses, increase the total losses of the system. From a system perspective, this is not a positive effect.

BESS increases the overall utilization time of the existing equipment and grid. BESS has a shorter lifetime, and there will be several reinvestments during the lifetime of a transformer. Due to the low investment costs of a transformer compared to a BESS, the BESS must be able to cover the investment cost with the total operational cost savings. The reinvests will be cheaper by time if the price projections of lower costs in the future are correct. The utilization of the existing grid of a highly fluctuating load is better compared to a more traditional load with a flatter power profile. This case study has a load where the power peaks and periods with high power are short-lasting. If BESS installations are more widespread in the future, the sum of peak shaving at the lowest level can postpone grid investment on higher grid levels.

If BESS is applied in the near future, BESS can be used as an alternative to grid reinforcement is potentially high. BESS can be installed with an initial SoH lower than one, i.e., reuse already used batteries from, for instance, EV batteries. Thus, looking at the whole

energy system, BESS applied for peak shaving can be a positive contributor to a circular economy and reduce overall costs.

However, BESS can be used for other grid services as well. As in [9], when the operator of the FCS is using the BESS for frequency control, the profitability increases, and it provides grid services for the transmission grid operator. In light of the increasing distribution of RES, applying BESS is smoothening out the grid power and reduce fluctuations from PV production [11]. BESS can contribute to realize a higher share of RES and contribute to reducing the carbon intensity of power production.

6.5 Model assumptions

The optimization model is based on several assumptions, which can be seen as advantages and disadvantages. All premises and simplifications will move the model from the ideal and realistic world. However, some of them are good to eliminate potential sources for interpretation. The case study with an EV FCS is based on a real FCS in Trøndelag, and this is input to the model. However, the model can take any load as input.

As mentioned in section 6.1, the significant cost savings are from power tariffs. Energy capacity is needed. However, it does not directly contribute to cost savings. It indirectly contributes because stored energy is needed to provide power from the BESS. The degradation mechanisms in the Master's thesis are only on capacity fade and not power fade.

The principle of one day representing one month must be discussed because it is the reason for several weaknesses of the model. The reason for the choice was due to computational force and the wish to analyze for a long term period (5 years) with time resolution in minutes. Each day had an operational cost, which was multiplied with the number of days in the month. The first disadvantage is that the variations within a month are not present. That is partly shown in table 4.2, where the annual energy difference from the estimated EV charging demand (365 days) and the input to the optimization model is 131 MWh. The difference is equal to 1 % of the total energy consumption. As a part of the discussion in section 6.1, the issue was touched when cost savings in July were a consequence of bought energy in June. It is a late discovered weakness and means that some BESS energy is given for "free". If at the end of the day (i.e., the day that represents the month) is 200 kWh and in the beginning 100 kWh, a net energy increase is present that day. The cost of buying energy is multiplied by the number of days that month. Thus the optimization will minimize these costs based on monthly variations in the spot price. In the ideal case, all the 365 days would be input. Since the spot price has monthly and daily fluctuations, which are following different patterns, this gives a small error in the cost of purchasing

electricity. The error is probably not a substantial effect since the spot cost element has a tiny difference in that case of comparing NPVs between BESS and grid reinforcement. However, it is present and is seen in figure 5.4, where July had a small cost saving. The reason is due to the model weakness as cost savings in July is from energy purchase in June, as discussed here and in section 6.1.

The optimization of the estimated EV charging demand and spot prices are known before solving. That is not the case in reality. The EV charging demand will depend on the number of cars when they arrive, and the initial SoC of the EV battery of the incoming vehicles. The spot price is varying on market conditions. The battery degradation is also assumed to have a constant temperature, which will not be the case. When the temperature is higher than expected, the calender aging will be accelerated while the cyclic degradation will be decelerated. The temperature will go up in reality due to time delays in the cooling system. A high battery power, thus high current, will cause heating. However, the BMS could measure current and based on that act accordingly and therefore have small temperature variations, but there will still some. Dynamic programming can control a BESS in real life and optimize the operation of the battery, such as suggested in [54]. Also, MCP algorithms are recommended to control BESS, for example, in [55] as a charge/discharge control scheme.

Chapter 7

Conclusion and further work

7.1 Conclusion

The conclusion will answer the problems formulated in chapter 1. In this thesis, a comparison between grid reinforcement and BESS installation is considered, and a case study has been conducted for an EV FCS. The case is based on today's situation and investigate the case if the number of chargers increases with 50 %. The objective of the BESS is to shave the power peaks of the EV charging demand. An optimization model implemented in Julia is built and used to optimize the operation and costs for a five year period. The transformer loss costs are not varying significantly for various BESS configurations. Installing the optimal BESS and keeping a 1250 kVA transformer results in higher losses compared to reinforcing the grid with a 1600 kVA transformer.

The results obtained from the optimization shows higher discounted costs for installing a BESS than reinforcing the grid. The optimal BESS configuration of 225 kWh and 300 kW in the case study cuts the peak power from the grid with 19 % and generate operational cost savings of 800 kNOK. Due to high investment costs, the alternative of reinforcing the grid is more profitable and has 900 kNOK less total cost. When installing a BESS, energy arbitrage gives small cost savings compared to the savings from reduced power tariff. From a grid perspective, there is no significant difference in energy losses or costs of energy losses.

The degradation did, in an almost insignificant manner, impact the total costs. The BESS was dimensioned based on the time period of 5 years and estimation of SoH after five years. To conclude on this, two main methods can be used to decide the necessary BESS

capacity to ensure low degradation impact after a specific time period. The first is to optimize without any degradation mechanisms and with the BESS size (maximum power and energy capacity) as variables. The battery capacity from optimization results is then divided with the assumed final SoH of the time period. Calender aging can be calculated and give a sufficient estimate of the closing SoH. The calender aging dominates the total degradation and can be calculated with only one operational information, which is temperature. The other method is to do optimization with degradation, which is computationally much heavier. The cost of degradation can and has been used in previous work for analyzing BESS. The extra investment cost due to the degradation, as concluded here, should be incorporated using an equivalent cost for degradation in the objective function to give a realistic cost estimate.

The spot sensitivity analysis shows that a random pick of spot prices gives an expected deviation from the average total operational cost of 1.14 %. The expected deviation can be understood as an expected potential, both in a negative and positive direction, for energy arbitrage.

The time step analysis shows that the total operational costs are 14.5 % higher when the time resolution is in minutes compared to hours. When cyclic aging is included, the SoH decrease 45 % faster when the resolution is in minutes. The reason for the faster SoH decline is due to the different number of FEC and not the average C-rate.

The last sensitivity analysis, which is on grid tariffs, shows that a more expensive grid tariff regime increases the cost savings for the BESS compared to grid reinforcement. The alternative grid tariffs made the NPV 6.7 % higher while the NPV difference between BESS and grid reinforcement decreased by 29 %. The DSO can do the optimization of the grid and optimize the tariff structure based on their wishes, which must be represented in the objective function.

In the end, the future battery investment costs projections will give a 54 % decrease in the NPV difference between BESS and grid reinforcement. With alternative grid tariffs, the reduction in NPV difference between BESS and grid reinforcement is 75 %.

7.2 Further work

The EV charging demand and spot prices are pre-known variables. An objective for further work is making an operating model for the BESS, where the algorithm must estimate the mentioned variables. An algorithm that predicts and determines these variables can be used in real life to control a BESS.

As mentioned, the power fade is not part of the degradation modeling. Adding that to the model will improve the complexity and wholeness. The driving cost saving when installing BESS is in the power tariffs. The impact of power fade is, therefore, essential to consider from an economic perspective.

The optimization model can be further improved in several ways. First, as mentioned, power fade can be added. Another improvement will be to include the BESS size in the objective function, which was initially intended in this thesis as well. In short, that will be to combine the two models, the calibration model and optimization model. In that way, the verification of the optimal solution will be more convenient. And last, remove the representation of a month with one day, such that the model includes the whole year with unique days. The two last-mentioned improvements could have been done in this thesis but were not due to computational limits.

The proposed optimization model can be applied to other grid applications and all types of load with a minute based power profile. The case studied in this thesis is not the ideal case for a BESS, since the investment costs for grid reinforcement was low. Other cases with weaker grid or long power lines are of a higher BESS profitability opportunity.

Bibliography

[1] Dag Spilde, Synne Krekling Lien, Ingrid Magnussen, and Torgeir Ericson. Energibruk i Norge mot 2035. PDF download available at: https://www.nve.no/nytt-fra-nve/nyheter-energi/elektrifisering-av-transport-gir-nedgang-i-samlet-energibruk/, 2018. NVE. Accessed: 2020-Feb-4.

[2] Christer Heen Skotland, Eirik Eggum, and Dag Spilde. Hva betyr elbiler for strømnettet? PDF download available at: https://www.nve.no/nytt-fra-nve/nyheter-energi/stromnettet-er-klar-for-elbilene/, 2016. NVE. Accessed: 2020-Feb-4.

[3] Andrew W. Thompson. Economic implications of lithium ion battery degradation for vehicle-to-grid (v2x) services. *Journal of power sources*, Vol. 396:pages 691–709, August 2018.

[4] Anthony Barré, Benjamin Deguilhem, Sébastien Grolleau, Mathias Gérard, Frédéric Suard, and Delphine Riu. A review on lithium-ion battery ageing mechanisms and estimations for automotive applications. *Journal of power sources*, Vol. 241:pages 680–689, June 2013.

[5] Wasim Sarwar. *Hybridised Energy Storage Systems for Automotive Powertrain Applications*. PhD thesis, Imperial College London, August 2016.

[6] Björn Nykvist and Måns Nilsson. Rapidly falling costs of battery packs for electric vehicles. *Nature Climate Change*, Vol. 5:pages 329–332, March 2015.

[7] M. A. Hannan, M. M. Hoque, A. Hussain, Y. Yusof, and P. J. Ker. State-of-the-art and energy management system of lithium-ion batteries in electric vehicle applications: Issues and recommendations. *IEEE Access*, Vol. 6:pages 19362–19378, March 2018.

[8] Andreas Poullikkas. A comparative over view of large-scale battery systems for electricity storage. *Renewable and sustainable energy reviews*, Vol. 27:pages 778–788, August 2013.

[9] Lucas Richard and Marc Petit. Fast charging station with battery storage system for EV: Grid services and battery degradation. In *2018 IEEE International Energy Conference (ENERGYCON)*, pages 1–6, June 2018.

[10] Lucas Richard and Marc Petit. Fast charging station with battery storage system for EV: Optimal integration into the grid. In *2018 IEEE Power & Energy Society General Meeting (PESGM)*, pages 1–5, August 2018.

[11] Frida Berglund. Department of electrical engineering – performance degradation modelling and techno-economic analysis of lithium-ion battery energy storage systems. Master's thesis, Department of electric power engineering, NTNU – Norwegian University of Science and Technology, June 2018.

[12] Paul van den Oosterkamp, Paul Koutstaal, Adriaan van der Welle, Jeroen de Joode, Jip Lenstra, Karel van Hussen, and Robert Haffner. The role of DSOs in a smart grid environment. URL: http://www.edsoforsmartgrids.eu/wp-content/uploads/public/EDSO-views-on-Data-Management-June-2014.pdf, April 2014. ECORYS report on mission from the European Commission.

[13] Eirik Haugen. Charging demand at electric vehicle fast charging station case study and lithium ion battery degradation literature review. Project report in TET4520, Department of electric power engineering, NTNU – Norwegian University of Science and Technology, December 2019.

[14] Arina Anisie and Francisco Boshell. Utility-scale batteries: Innovation landscape brief, 2019. International renewable energy agency - Innovation team at IRENA's Innovation and Technology Centre.

[15] International renewable energ. Electricity storage and renewables: Costs and markets to 2030, 2017. Review and forecast on energy storage and renewables to 2030.

[16] Wajahat Khan, Furkan Ahmad, and Mohammed Saad Alam. Fast EV charging station integration with grid ensuring optimal and quality power exchange. *Engineering science and technology, an international journal*, Vol. 22:pages 143–152, August 2018.

[17] Johann Walter Kolar. Power electronic system II. ETH Zürich, 2018. Lecture notes.

[18] Maik Naumann. *Techno-economic evaluation of stationary battery energy storage systems with special consideration of aging*. PhD thesis, Technische Universität München, July 2018.

[19] Samppa Jenu, Aino Menninen, Saara Tuurala, and Ari Hentunen. Simplified state of health diagnostics tool. *Invade Horizon 2020 Deliverable 6.3*, 2018.

[20] Xiangping Chen and Wenping Cao. *Advancements in Energy Storage Technologies*. IntechOpen, 2018. ISBN 978-1-83881-346-8.

[21] Eduard Ignatev. Optimal operation of battery storage for peak shaving applications. Master's thesis, Lappeenranta University of Technology, 2016.

[22] Florian Wankmüller, Prakash R. Thimmapuram, Kevin G. Gallagher, and Audun Botterud. Impact of battery degradation on energy arbitrage revenue of grid-level energy storage. *Journal of energy storage*, Vol. 10:pages 56–66, April 2017.

[23] Maik Naumann, Cong Nam Truong, Michael Schimpe, Daniel Kucevic, Andreas Jossen, and Holger C. Hesse. SimSES: Software for techno-economic simulation of stationary energy storage systems. In *International ETG Congress 2017, Bonn, Germany*, pages pages 1–6, November 2017.

[24] Kandler Smith, Matthew Earlywine, Eric Wood, Jeremy Neubauer, and Ahmad Pesaran. Comparison of plug-in hybrid electric vehicle battery life across geographies and drive-cycles. In *SAE World Congress and Exhibition, April 24-26, 2012, Detroit, Michigan*. U.S. Deparment of Energy, April 24-26 2012.

[25] Philippe Gyan, Philippe Aubret, Julien Hafsaoui, Franck Sellier, Sandrine Bourlot, Stephane Zinola, and Francois Badin. Experimental assessment of battery cycle life within the simstock research program. *Oil & Gas Science and Technology*, Vol. 68: pages 137–147, February 2013.

[26] John Wang, Justin Purewal, Ping Liu, Jocelyn Hicks-Garner, Souren Soukazian, Elena Sherman, Adam Sorensen, Luan Vu, Harshad Tataria, and Mark W. Verbrugge. Degradation of lithium ion batteries employing graphite negatives and nickelecobaltemanganese oxide beta spinel manganese oxide positives: Part 1, aging mechanisms and life estimation. *Journal of power sources*, Vol. 269:pages 937–948, December 2014.

[27] Andrea Cordoba-Arenas, Simona Onori, Yann Guezennec, and Giorgio Rizzoni. Capacity and power fade cycle-life model for plug-in hybrid electric vehicle lithium-ion battery cells containing blended spinel and layered-oxide positive electrodes. *Journal of Power Sources*, Vol. 278:pages 473 – 483, March 2015.

[28] Michele de Gennaro, Elena Paffumi, Giorgio Martini Andrew Giallonardo, Samuel Pedroso, and Aaron Loiselle-Lapointe. A case study to predict the capacity fade of the battery of electrified vehicles in real-world use conditions. *Case studies on transport policy*, November 2019.

[29] Willett Kempton and Jasna Tomic. Vehicle-to-grid power fundamentals: Calculating capacity and net revenue. *Journal of power sources*, Vol. 144:pages 268–2797, June 2005.

[30] Peter Achin, Kjersti Berg, Idar Petersen, and Pedro Crespo del Granado. Når er batterier lønnsomme? pages 1–2. SINTEF Energi AS, 2019.

[31] Ryan Hledik, Judy Chang, Roger Lueken, Johannes Pfeifenberger, John Imon Pedtke, and Jeremy Vollen. The economic potential for energy storage in nevada. URL: www.energy.nv.gov/, 2018. Prepared for: Public Utilities Commission of Nevada Nevada Governor's Office of Energy.

[32] Wesley Cole and A. Will Frazier. Cost projections for utility-scale battery storage. URL: www.nrel.gov/docs, 2019. U.S. national renewable energy labratory.

[33] X-rate (home web site): average exchange rates. URL: www.x-rates.com/average, 2019. Accessed: 2020-Apr-20.

[34] Michał Pióro and Deepankar Medhi. Chapter 5 - general optimization methods for network design. In Michał Pióro and Deepankar Medhi, editors, *Routing, Flow, and Capacity Design in Communication and Computer Networks*, The Morgan Kaufmann Series in Networking, pages pages 151 – 210. Morgan Kaufmann, San Francisco, 2004.

[35] Khan Academy. Lagrange multipliers, examples. URL: https://www.khanacademy.org/math/multivariable-calculus/applications-of-multivariable-derivatives/constrained-optimization/a/lagrange-multipliers-examples, 2020. Accessed: 2020-May-29.

[36] Peter Moles and Nicholas Terry. *The Handbook of International Financial Terms*. Oxford, 1 edition, 1997. ISBN 9780191727245.

[37] Nord Pool. Intraday market. URL: https://www.nordpoolgroup.com/the-power-market/Intraday-market/, 2020. Accessed: 2020-May-29.

[38] Tarjei Kristiansen. Pricing of monthly forward contracts in the Nord Pool market. *Energy Policy*, Vol. 35:pages 307–316, February 2007.

[39] Tensio. Nettleiepriser 2020 – for næring og offentlige virksomheter. URL: https://tn.tensio.no/kunde/nettleie/priser, 2020. Accessed: 2020-Apr-8. PDF file.

[40] Hafslund. Factors influencing grid tariffs. URL: www.hafslundnett.no, 2020. Accessed: 2020-Jan-21.

[41] Olje- og energidepartementet. Lov om produksjon, omforming, overføring, omsetning, fordeling og bruk av energi m.m. (energiloven). URL: https://lovdata.no/dokument/NL/lov/1990-06-29-50, 2009. Accessed: 2020-Jan-31.

[42] Mirna Grzanic, Tomislav Capuder, and Slavko Krajcar. DSO and aggregator sharing concept for distributed battery storage system. In *2018 IEEE International Conference on Environment and Electrical Engineering and 2018 IEEE Industrial and Commercial Power Systems Europe (EEEIC / I&CPS Europe)*, pages 1–6, June 2018.

[43] Kjell Sand. Samfunnsøkonomiske tapskostnader for dimensjonering av kraftnett kostnadsnivå 2014. *SINTEF Energi. Report*, 2014. Report number: TR A7346.

[44] Nina Wahl Gundersen. Technical-economic analysis of fast chargers for plug-in electric vehicles in distribution networks. Master's thesis, Department of electric power engineering, NTNU – Norwegian University of Science and Technology, June 2010.

[45] SSB - Statistics Norway. Electricity balance (GWh) for Norway 2018. URL: www.ssb.no/en/energi-og-industri/statistikker/elektrisitet, 2019. Accessed: 2020-May-9.

[46] Håkon Tjelmeland. Temaside for TMA4240/TMA4245 statistikk: Deskriptiv statistikk. URL: www.wiki.math.ntnu.no, 2017. NTNU.

[47] The julia programming language. URL: www.julia.org, 2017. Julia web site.

[48] Andreas Wächter. Short tutorial: Getting started with ipopt in 90 minutes. In *Combinatorial Scientific Computing*, 2009.

[49] M. A. Hannan, M. M. Hoque, A. Hussain, Y. Yusof, and P. J. Ker. State-of-the-art and energy management system of lithium-ion batteries in electric vehicle applications: Issues and recommendations. *IEEE Access*, Vol. 6:pages 19362–19378, 2018.

[50] Seung-Yeong Yu, Hyun-Jun Kim, Jae-Hyuk Kim, and Byung-Moon Han. SoC-based output voltage control for BESS with a lithium-ion battery in a stand-alone DC microgrid. *Concept paper*, November 2016.

[51] Ari Hentunen, Juha Forsström, Samppa Jenu, Saara Tuurala, Aino Manninen, and Sigurd Bjarghov. Battery techno-economic tool. *Invade Horizon 2020 Deliverable 6.2*, 2018.

[52] Hafslund. Grid tariffs prices. URL: www.hafslundnett.no, 2020. Accessed: 2020-Jan-15.

[53] NVE. RME høringsdokument - endringer i nettleiestrukturen. PDF download available at: https://www.nve.no/reguleringsmyndigheten/nytt-fra-rme/saker-pa-horing-reguleringsmyndigheten-for-energi-rme/horing-forslag-til-endringer-i-utformingen-av-nettleien/?fbclid=IwAR137uyE-IVYO6Phua8hYnm044HQFWeWUg8UNXD1nyclbp9lNCbuIzdGUdE, 2020. Accessed: 2020-May-28.

[54] Philipp Fortenbacher, Johanna L. Mathieu, and Göran Andersson. Modeling, identification, and optimal control of batteries for power system applications. *Power Systems Computation Conference, Wroclaw*, pages 1–7, 2014.

[55] Satoru Akagi, Shinya Yoshizawa, Masakazu Ito, Yu Fujimoto, Teru Miyazaki, Yasuhiro Hayashi, Katsuhisa Tawa, Toshiya Hisada, and Takashi Yano. Multipurpose control and planning method for battery energy storage systems in distribution network with photovoltaic plant. *International Journal of Electrical Power & Energy Systems*, Vol. 116:pages 105485, September 2019.

Appendices

Appendix A

Method to estimate EV charging demand at FCS

The central development of the method to estimate EV charging demand was in the fall. The appendix will describe the details of the method. Figure A.1 shows the general method.

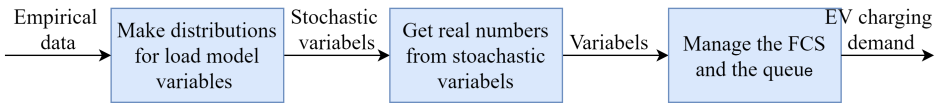

Figure A.1: Overall method to estimate EV charging demand [13].

First, empirical information is collected. The empirical data is input to generate expectation values for probability distributions. Then, the allocation of random numbers to variables based on their distributions for each time step. These numbers then determine all the necessary information to generate a power profile for the total charging demand at the FCS.

To make an intuitive approach explaining the model, imagine a FCS where a car has just arrived and started to charge. The time to the next arrival of a vehicle is exponentially distributed, with the expected value of X. The X is picked based on a non-homogenous Poisson distribution, which means that the expected value of the Poisson distribution varies with time, which describes the number of cars arriving each hour. This expected value of the Poisson distribution based on empirical charging data from Norway gives the hourly

patterns. The distribution of interarrival time between two Poisson distributed events is exponential. These are the factors and distributions which determine the traffic at the FCS.

When an EV arrives, it has a specific charging power and battery size, as well as an original EV battery SoC. The initial SoC was calculated based on another empirical distribution, which was the log-normally distributed vehicle kilometers traveled. By assuming a constant relationship between the driven distance and the driving range of the EV's, the initial SoC has a correlating distribution. The initial SoC of incoming EV's was, therefore, log-normal distributed with fixed expectation values and standard deviations based on the empirical data.

The incoming EV was allocated a specific battery size and charging power. The basis of the allocation was a clustered composition of the top ten EV models in the Norwegian EV park in fall 2019. The primary assumption was that the FCS was in a rural area, so the models with driving ranges below 200 km were omitted. The clustered groups consist of the six remaining EV models, where each group had a charging power and battery size. Each group has a total amount of cars and a fraction of the whole car park each. So group a was 9.2 % of the clustered total with a battery size of 80 kWh and charging power of 200 kW, and similar for group b and c. The arriving car in the model had a charging power and battery size from a uniform distribution, which corresponded to these fractions of the clustered groups.

Appendix B

Linear approximation of temperature dependent C-rate function

In chapter 3.2.2 the $f_c(T_K, C_r) = (a \cdot T_K^2 + b \cdot T_K + c)e^{(d \cdot T_K + e) \cdot C_r(t)}$ is said to be linearized. The linearization is done in this appendix, and the corresponding constants, $k_{C_{r0}}$ and $k_{C_{r1}}$, are computed. Taylor expansion is used to linearize the exponential function. The constants a, b, c, d and e are taken from table 2.3.

Taylor approximation of the exponential function $e^{k \cdot x}$ around the point x_0 is

$$e^{k \cdot x} = e^{k \cdot x_0} \sum_{n=0}^{N} \frac{k^n (x - x_0)^n}{n!}$$

For the linear case, N is set to 1 and

$$e^{k \cdot x} = e^{k \cdot x_0} \cdot (1 + k \cdot (x - x_0)) \tag{B.1}$$

By letting $k_C = (d \cdot T_K + e)$ and $x = C_r$, the exponential term $e^{(d \cdot T_K + e) \cdot C_r(t)}$ in f_c can be described with equation B.1 as $f_{lin}(T_K, C_r) = e^{k_C(T_K) \cdot C_r} = e^{k_C(T_K) \cdot C_r} \cdot (1 + k_C(T_K) \cdot (C_r - C_{r0}))$. By defining $k_{cyc}(T_K) = (a \cdot T_K^2 + b \cdot T_K + c)$, the function f_c now consists of a product of two temperature dependent functions and one C-rate dependent function,

and is as shown in equation B.2.

$$f_c(T, C_r) = k_{cyc}(T_K) \cdot f_{lin}(T_K, C_r) \tag{B.2}$$

To make f_c linear, the temperature cannot be a variable. Since f_{lin} is a linearized function with respect to C_r, f_c will be linear with respect to C_r. To capture this in the optimization, the factor $f_c(T_K, C_r(t))$ in equation 3.10 is split up in two parts, one constant and one linear with the C-rate. The constants depends on the temperature.

By setting the temperature T_K to a constant value T_0=5°C = 278 K, $k_{cyc} = 2.28{\cdot}10^{-3}$. The first order Taylor expansion of $e^{0.3869 \cdot C_r(t)}$ around $C_{r0} = 1.0\frac{1}{h}$ is $e^{0.4874 \cdot 1} \cdot (1 + 0.4874 \cdot (C_r(t) - 1.0)) = 1.6281 + 0.7935 \cdot (C_r(t) - 1.0)$. In total, f_c becomes

$$f_c(T_0, C_r) = 2.28 \cdot 10^{-3} \cdot \Big[1.6281 + 0.7935 \cdot (C_r(t) - 1.0)\Big] \tag{B.3}$$

$$= 1.903 \cdot 10^{-3} + 1.809 \cdot 10^{-3} \cdot C_r(t) \tag{B.4}$$

$$= k_{C_{r0}} + k_{C_{r1}} \cdot C_r(t) \tag{B.5}$$

The function f_c has a unit of measurement of % per FEC. For instance, 2000 full cycles with a constant C-rate of 1, gives a cyclic degradation of 7.4 %.

Appendix C

Interior point method

The interior point method is a way to compute an optmization problem by adding a barrier function to the objective function to ensure not avoiding the feasible region. Ipopt, and typically, the barrier function is defined as $\zeta \sum_{i=1}^{n} ln(s_i)$, including the variables $x_1, x_2, \ldots, x_n$ and a barrier parameter ζ. That definition is an approximation to fulfill the ideal properties, which are that the value of the barrier function is 0 when $g(x) \leq 0$ and ∞ when $g(x) > 0$. If the original problem on a general form is

$$\begin{aligned} \underset{x}{\text{minimize}} \quad & f(x) \\ \text{subject to} \quad & h(x) = 0 \\ & g(x) \leq 0 \\ & x \geq 0 \end{aligned}$$

the problem becomes

$$\begin{aligned} \underset{x}{\text{minimize}} \quad & f(x) - \zeta \sum_{i=1}^{n} ln(s_i) \\ \text{subject to} \quad & h(x) = 0 \\ & g(x) + s \leq 0 \\ & x \geq 0 \\ & s > 0 \end{aligned}$$

The approximations of the barrier function demand that it must be twice differentiable. A large ζ makes the approximation less accurate than for a smaller value of ζ. A low value of ζ improves the approximation. However, it makes the minimization by Newton Raphson's method difficult because the Hessian will have huge variations near the boundaries of the feasible set.

Appendix D

Mathematical formulation of the implemented optimization model

The appendix contains the implemented version of the optimization problem. The variable and parameter description is in section 3.1. The added vector d_m is giving the days in a month number for the corresponding time variable, both h by using the convertation function $h2t$ and t. The first 1440 elements of d_m has value 31, because January has 31 days, the next 1440 elements has value 28 because February has 28 days and so on. The transformation function $h2t$ is

$$h2t(h) = (h-1) \cdot 60 + 1 \tag{D.1}$$

$$\begin{aligned} \underset{\substack{P_{grid}^{max},\\ P_B^{max}, E_{B0}}}{\text{minimize}} \quad & C_{tot} = \sum_{y \in Y} \alpha(y) \Big[\sum_{h \in H} E_{grid}(h) \Big(c_{spot}(h) + c_{E,tar}(m) \Big) \cdot d_m(h2t(h)) \\ & + \sum_{m \in M} c_{P,tar}(m) \cdot P_{grid}^{max}(m) \Big] \end{aligned}$$

$$\text{subject to} \quad P_L(t) = P_{grid}(t) + P_B(t) \qquad \forall t \in T \tag{D.2a}$$

$$P_B(t) = P_{dchar}(t) - P_{char}(t) \qquad \forall t \in T \tag{D.2b}$$

$$\Delta E_B(t) = \eta_c \cdot P_{char}(t)\Delta t - \frac{1}{\eta_d} \cdot P_{dchar}(t)\Delta t \qquad \forall t \in T \tag{D.2c}$$

$$E_{B,cap} = SoH(t) \cdot E_{B0} \qquad \forall t \in T \qquad \text{(D.2d)}$$

$$SoC(t) = \frac{E_B(t)}{E_{B,cap}} \qquad \forall t \in T \qquad \text{(D.2e)}$$

$$C_r(t) = \frac{P_B(t)}{E_{B0}} \qquad \forall t \in T \qquad \text{(D.2f)}$$

$$SoH(t) = SoH(t_0) - k_t \cdot \sqrt{t} - f_c(t) \cdot FEC(t) \qquad \forall t \in T \qquad \text{(D.2g)}$$

$$\Delta FEC(t) = \frac{1}{2} \cdot \frac{P_{char}(t) + P_{dchar}(t)}{E_{B0} \cdot (SoC_{max} - SoC_{min})} \cdot d_m(t) \quad \forall t \in T \qquad \text{(D.2h)}$$

$$f_c(t) = k_{C_r0} + k_{C_r1} \cdot C_r(t) \qquad \forall t \in T \qquad \text{(D.2i)}$$

$$P_{char}(t) \leq P_{inv}^{max} \qquad \forall t \in T \qquad \text{(D.2j)}$$

$$P_{dischar}(t) \leq P_{inv}^{max} \qquad \forall t \in T \qquad \text{(D.2k)}$$

$$SoC(t) \geq SoC_{min} \qquad \forall t \in T \qquad \text{(D.2l)}$$

$$SoC(t) \leq SoC_{max} \qquad \forall t \in T \qquad \text{(D.2m)}$$

$$SoH(t) \geq SoH_{min} \qquad \forall t \in T \qquad \text{(D.2n)}$$

$$SoH(t) \leq SoH_{max} \qquad \forall t \in T \qquad \text{(D.2o)}$$

$$P_{grid}(t) \leq P_{grid}^{contract} \qquad \forall t \in T \qquad \text{(D.2p)}$$